The Abdus Salam
International Centre for Theoretical Physics

United Nations
Educational, Scientific and
Cultural Organization

IAEA
International Atomic Energy Agency

2028-10

Joint ICTP/IAEA Workshop on Atomic and Molecular Data for Fusion

20 - 30 April 2009

The Use of Atomic Data in Collisional-Radiative Modeling

Joe ABDALLAH

Los Alamos National Lab.
Group T4, MS B212
Los Alamos
USA

Strada Costiera 11, 34014 Trieste, Italy - Tel. +39 040 2240 111; Fax +39 040 224 163 - sci_info@ictp.it, www.ictp.it

THE USE OF ATOMIC DATA IN COLLISIONAL-RADIATIVE MODELING

JOE ABDALLAH

LOS ALAMOS NATIONAL LABORATORY

Workshop on Atomic and Molecular Data for
Fusion Energy Research

April 20 – 24, 2009

ICTP, Trieste, Italy

Los Alamos

THE USE OF ATOMIC DATA IN COLLISIONAL-RADIATIVE MODELING

- Introduction and motivation
- Atomic Physics Data
- Collisional-Radiative Modeling-Methods
- Radiation Properties of Plasmas
- Opacity

Los Alamos

What are plasmas?

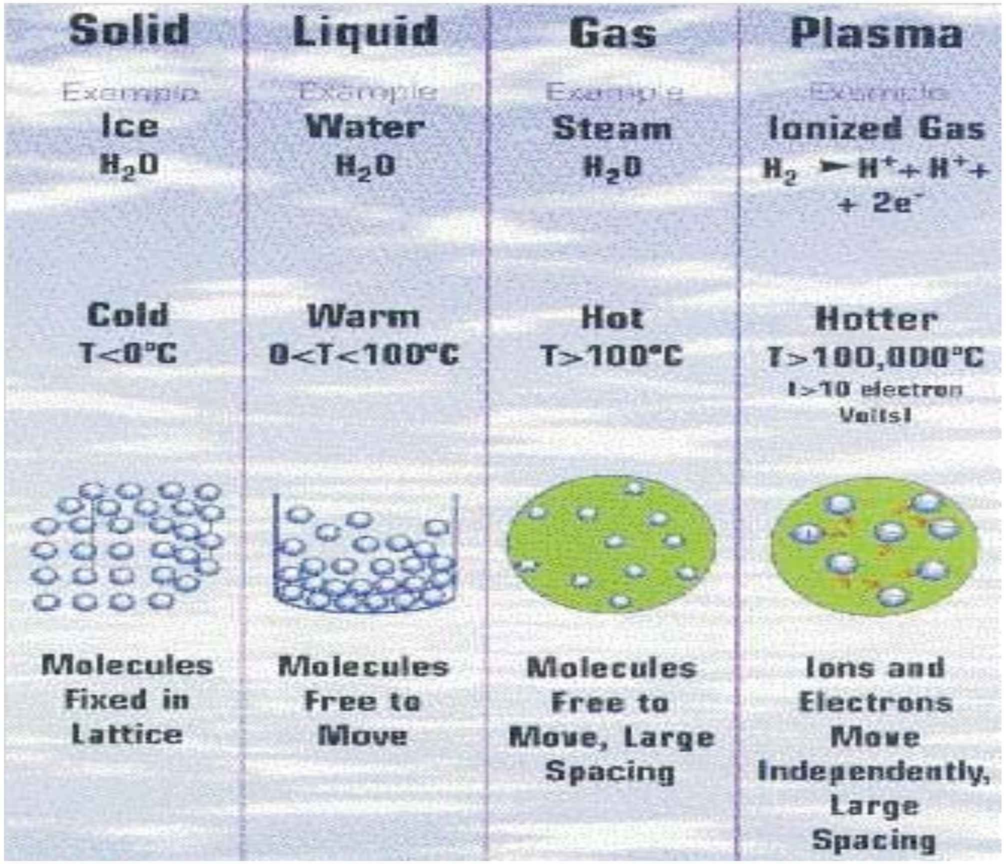

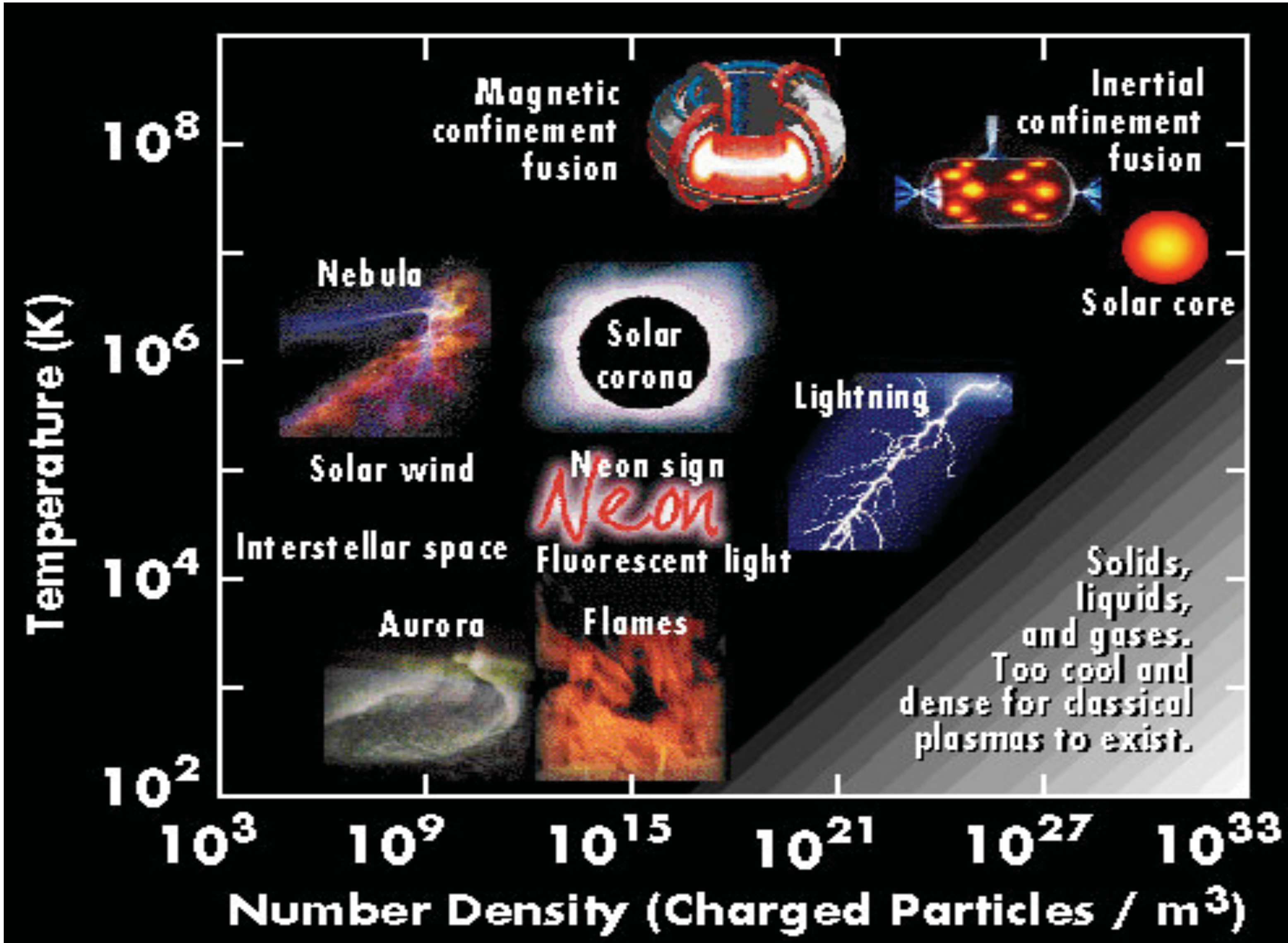
Magnetic confinement fusion
Inertial confinement fusion
Solar core
Nebula
Solar corona
Lightning
Solar wind
Neon sign
Neon
Interstellar space
Fluorescent light
Aurora
Flames
Solids, liquids, and gases. Too cool and dense for classical plasmas to exist.
Temperature (K)
10^8
10^6
10^4
10^2
10^3
10^9
10^15
10^21
10^27
10^33
Number Density (Charged Particles / m^3)

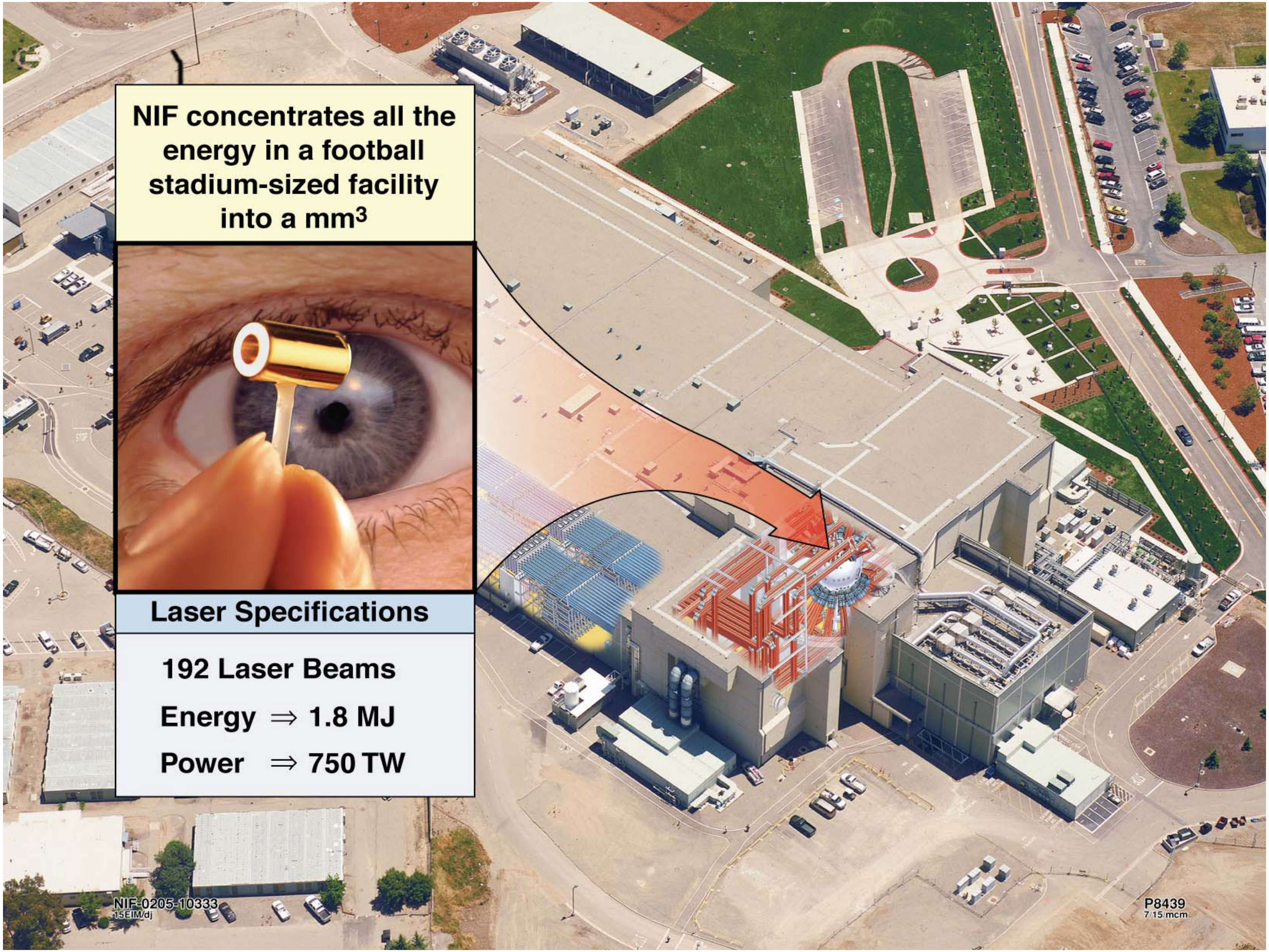
NIF concentrates all the energy in a football stadium-sized facility into a mm3
Laser Specifications
192 Laser Beams
Energy ⇒ 1.8 MJ
Power ⇒ 750 TW
NIF-0205-10333
15EIM/dj
P8439
7/15/mcm

NIF is 80% complete
NIF-0905-11317
01EIM/dj
E. Moses – WP3.2 P9687

The Most Successful Magnetic Confinement Configuration is the Tokamak

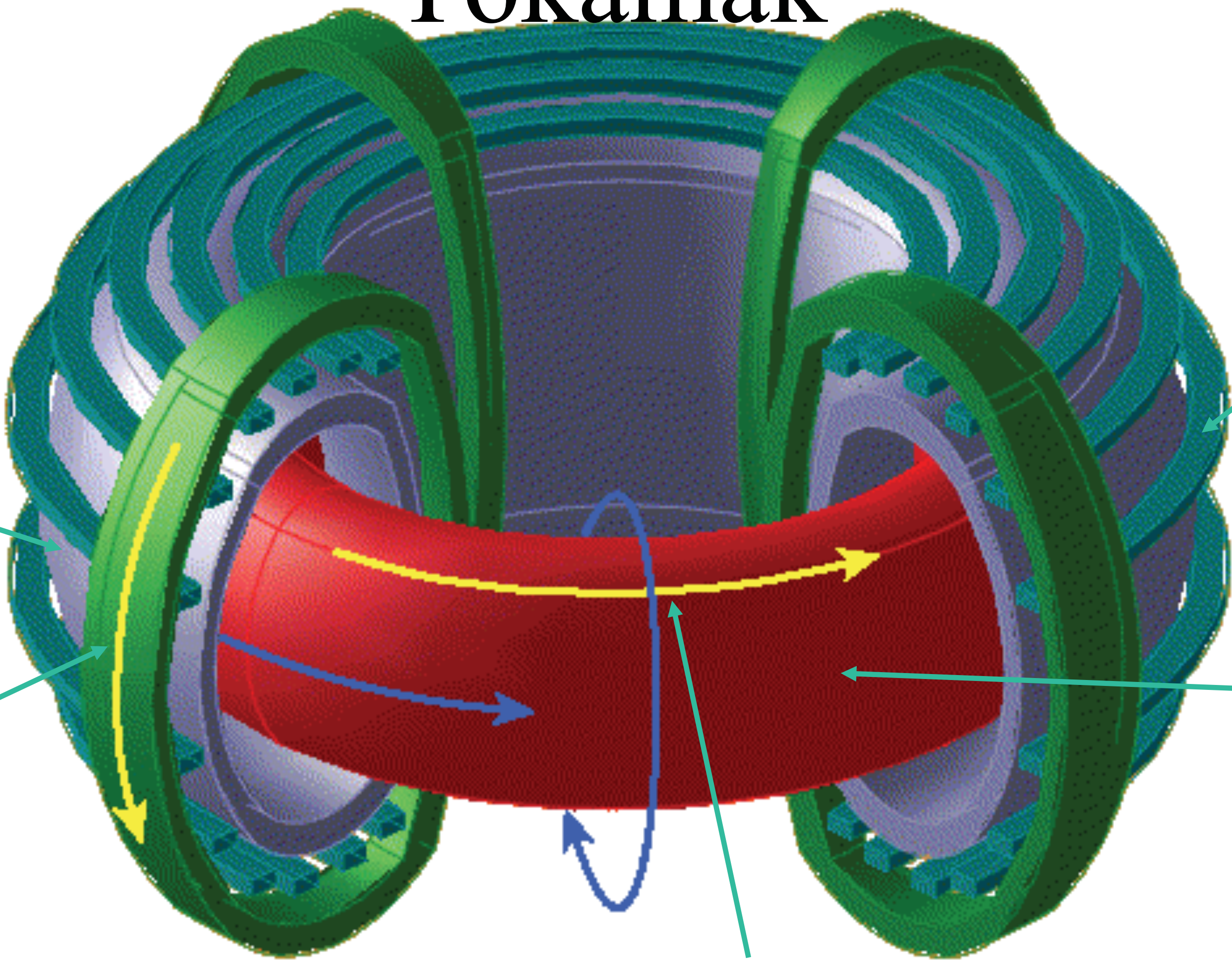

The Largest Tokamak Is the Joint European Torus in England

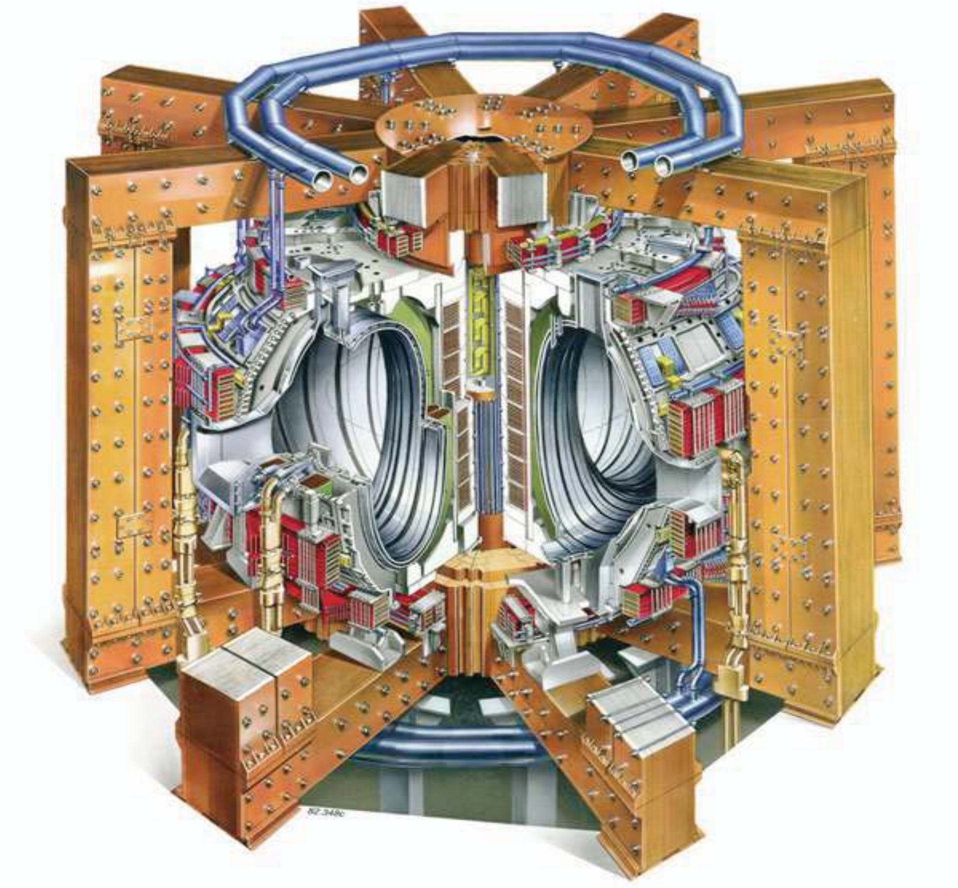

cutaway drawing

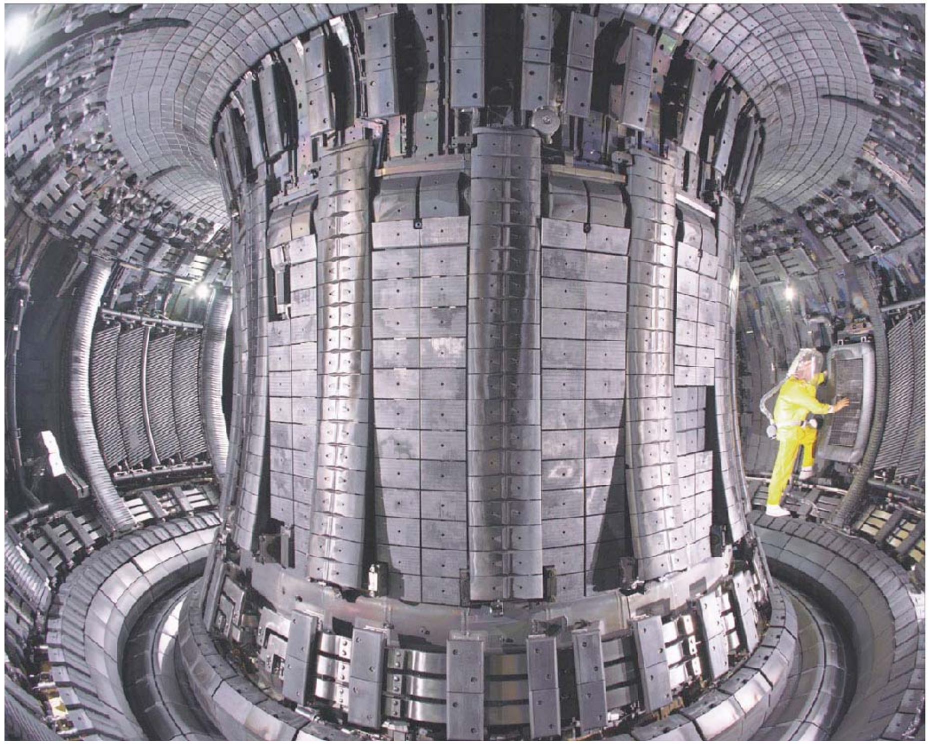

view of inside during maintenance

Working Tokamaks Are Usually Hidden by Support Systems & Diagnostics

The 20million Amp current provided by the Z accelerator enables this research

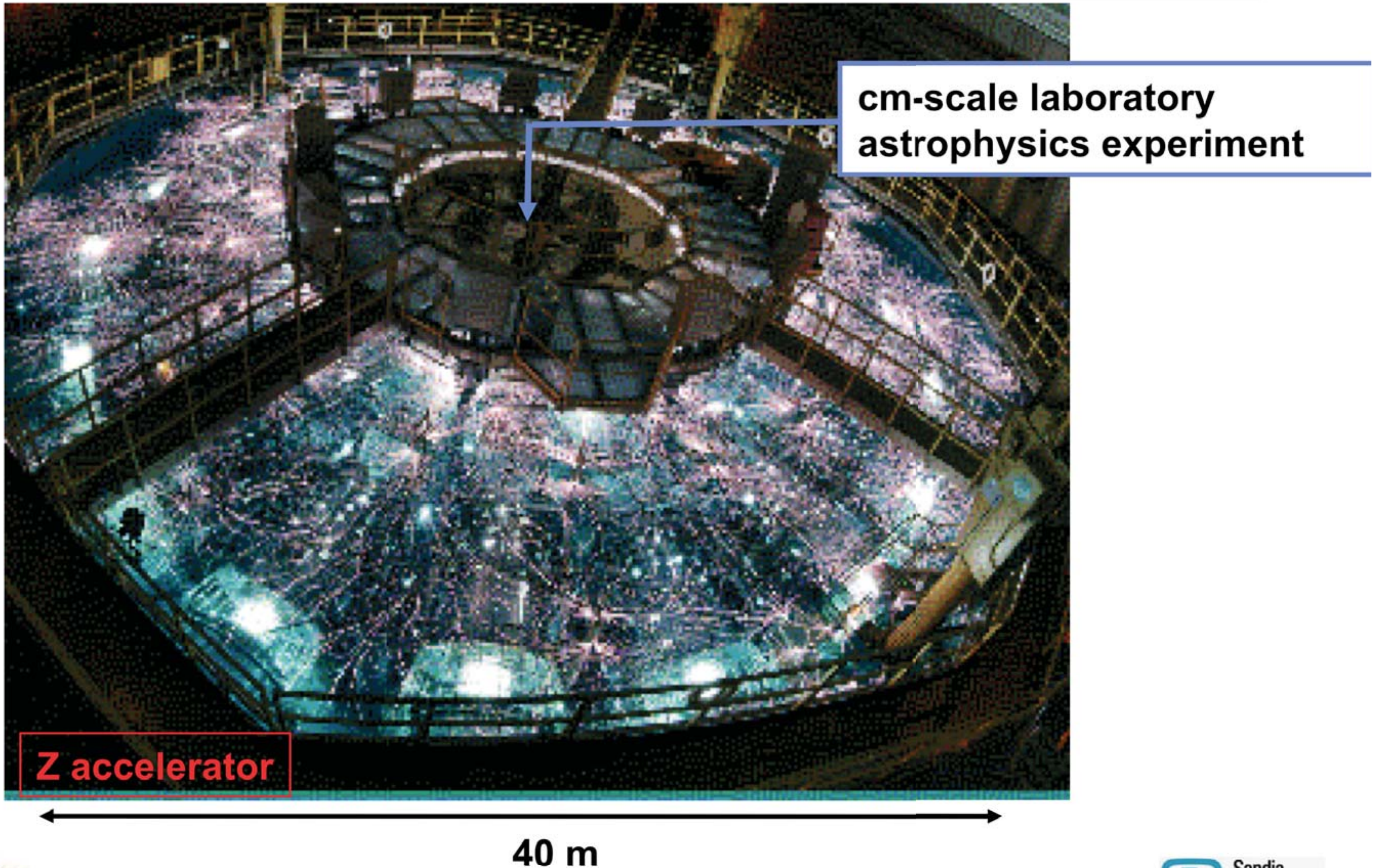

Sandia National Laboratories

LLNL Electron Beam Ion Trap (EBIT):
Atomic Physics Experiments on highly ionized heavy atoms

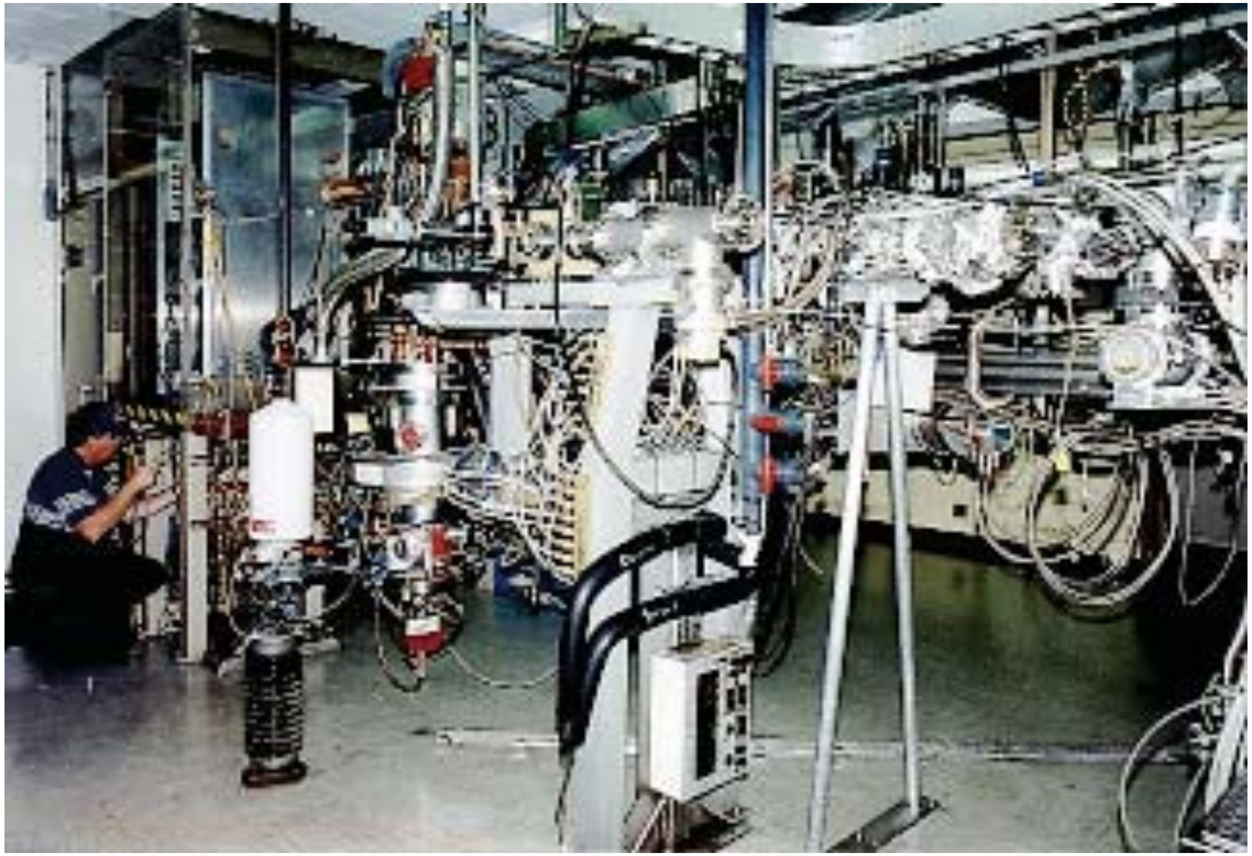

LAPD/UCLA

He Gas jet experiments, *TRIDENT LASER*

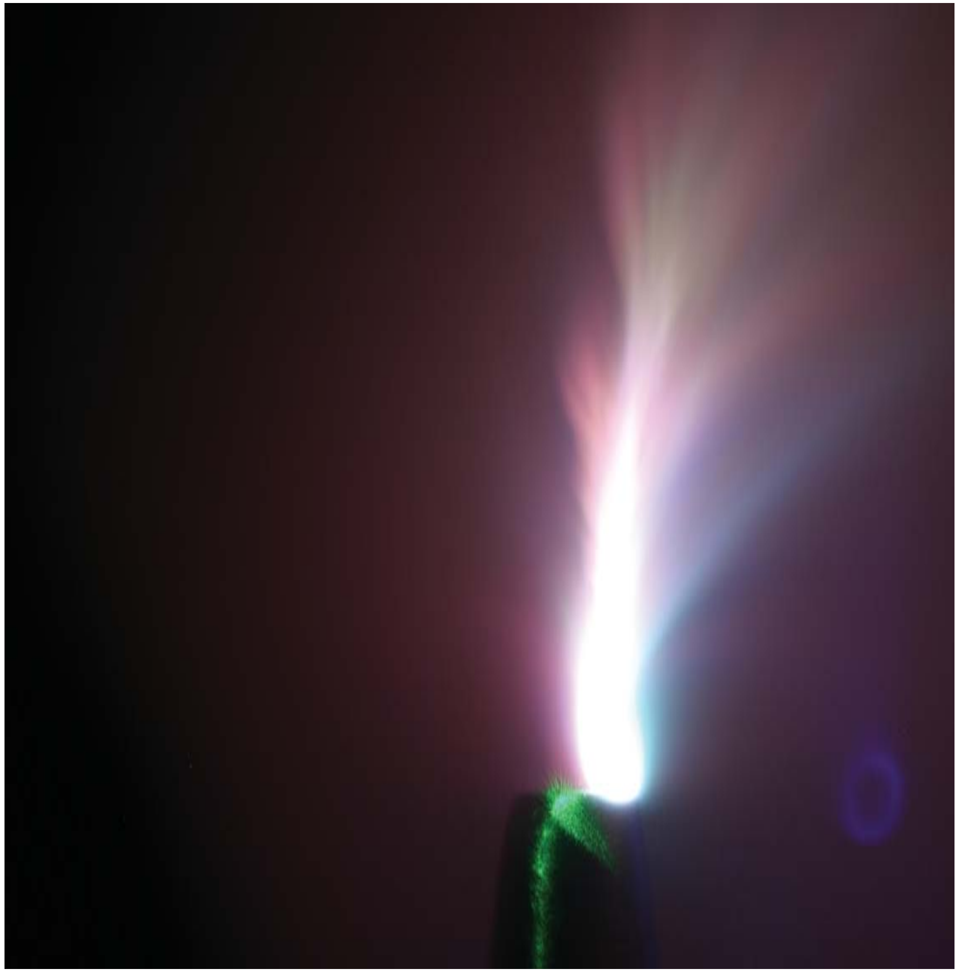

Los Alamos

Why Collisional-Radiative (CR) Modeling?

- Plasmas emit and absorb electromagnetic radiation.
- **CR** models provide atom/ ion state populations that are required to simulate radiation properties of plasmas.
- **CR** calculations provide diagnostic information about plasma conditions, e.g. , density and temperature by comparison with experiment.
- **CR** include electron collisions which are generally responsible for populating excited states.

He-like and H-like Al lines from a laser produced plasma

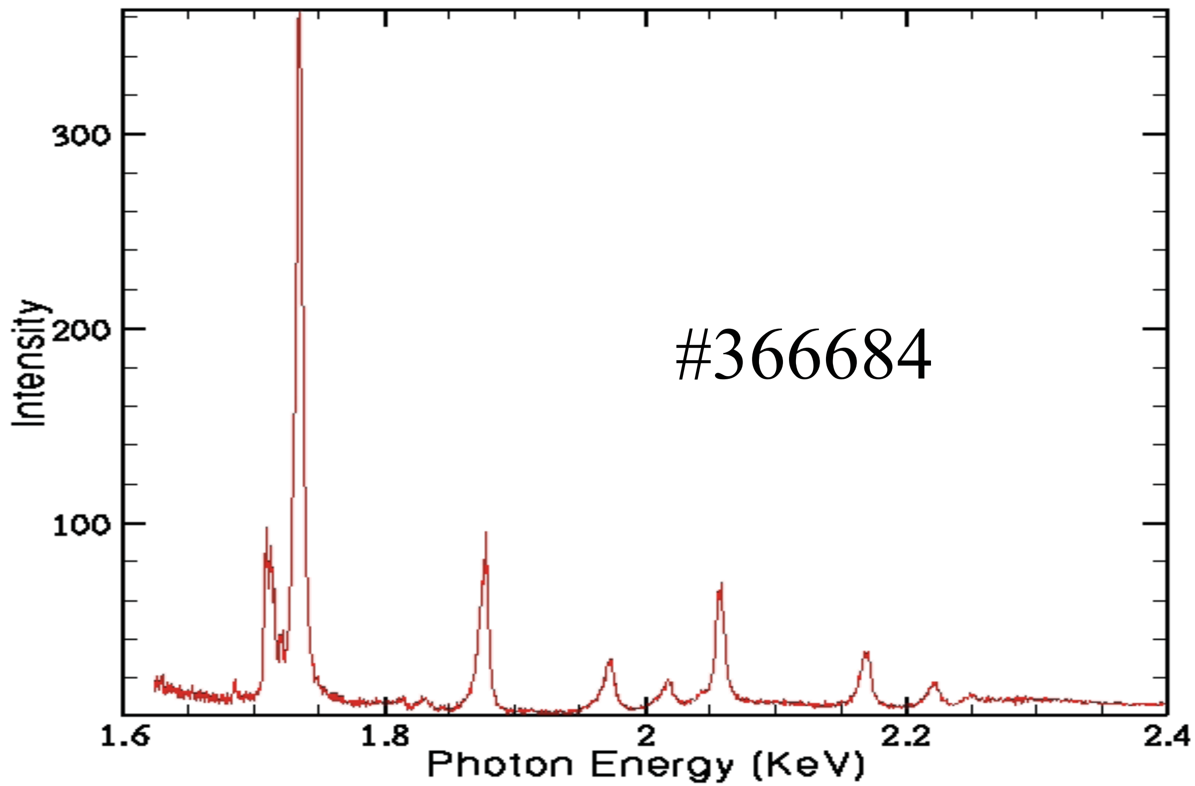

Notation for Electron Configurations

set of orbitals $(nl)^w$

n = principle quantum number

$n = 1,2,3,\ldots$

l = angular momentum quantum number

$l = 0,1,2,3,\ldots,n$

designated by spectroscopic notation $spdf$

w = occupation number(number of electrons in orbital)

maximum value of $4l + 2$

Example, ground configuration of nitrogen :

$1s^2 2s^2 2p^3$

Block Diagram NeI

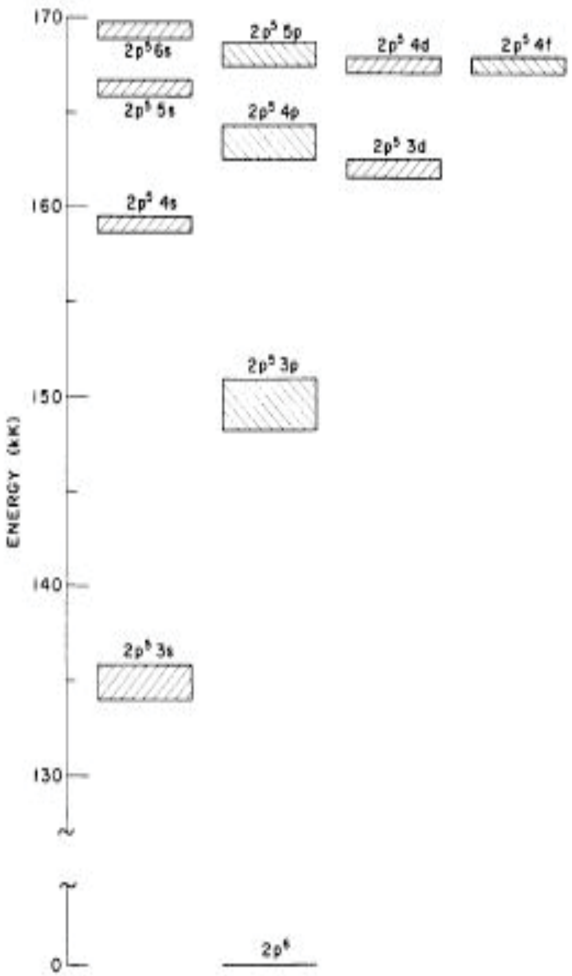

Energy level structure of *pd* configuration

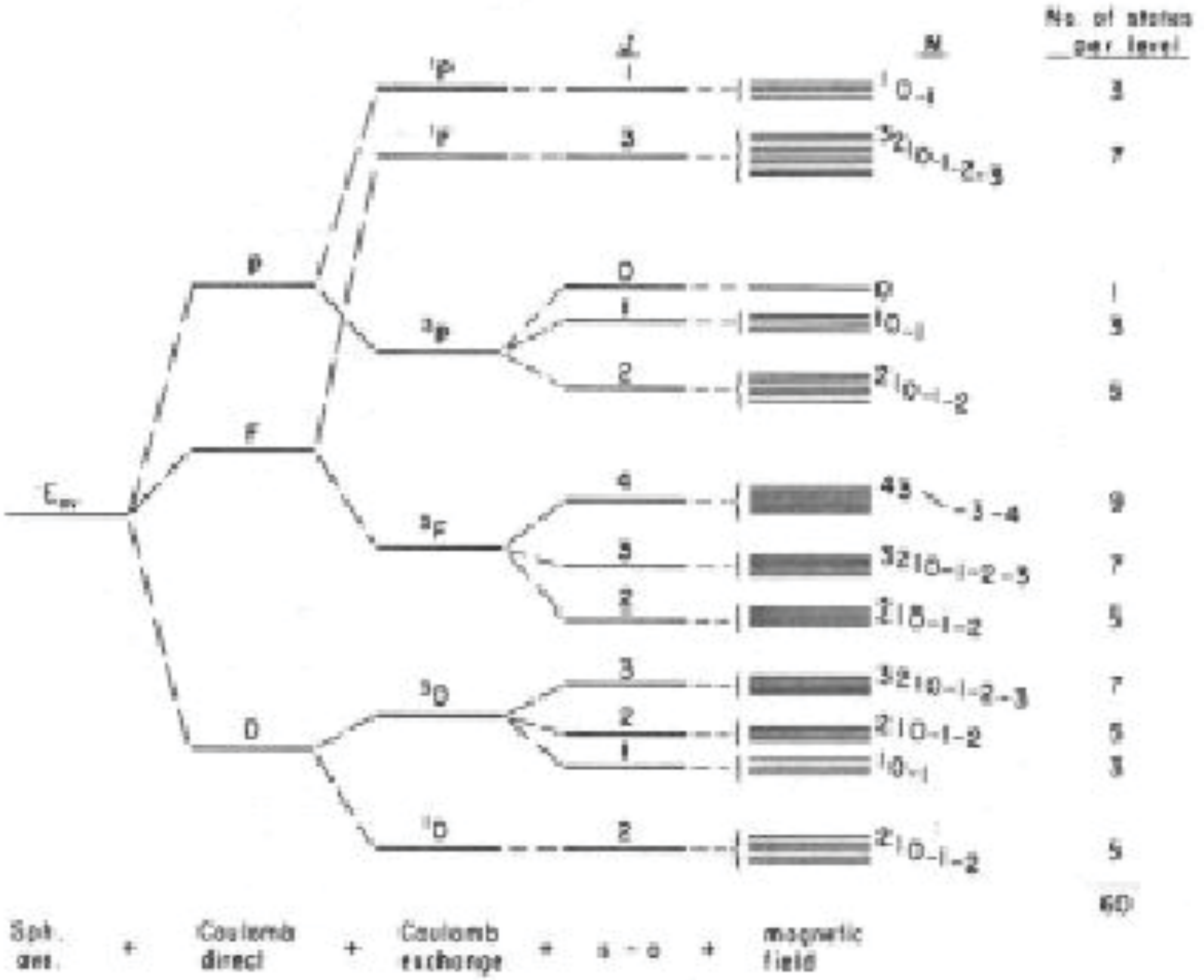

TABLE 4-2. PERMITTED LS TERMS FOR s^w, p^w, d^w, and f^w SUBSHELLS[a]. The subscripts indicate the number of different terms having the same values of LS. (Odd-parity superscripts omitted for brevity.)

					Total Number
s	^2S				1
s^2	^1S				1
p, p^5	^2P				1
p^2, p^4	$^1(SD)$	^3P			3
p^3	$^2(PD)$	^4S			3
d, d^9	^2D				1
d^2, d^8	$^1(SDG)$	$^3(PF)$			5
d^3, d^7	$^2(PD_2FGH)$	$^4(PF)$			8
d^4, d^6	$^1(S_2D_2FG_2I)$	$^3(P_2DF_2GH)$	^5D		16
d^5	$^2(SPD_3F_2G_2HI)$	$^4(PDFG)$	^6S		16
f, f^{13}	^2F				1
f^2, f^{12}	$^1(SDGI)$	$^3(PFH)$			7
f^3, f^{11}	$^2(PD_2F_2G_2H_2IKL)$	$^4(SDFGI)$			17
f^4, f^{10}	$^1(S_2D_4FG_4H_2I_3KL_2N)$	$^3(P_3D_2F_4G_3H_4I_2K_2LM)$	$^5(SDFGI)$		47
f^5, f^9	$^2(P_4D_5F_7G_6H_7I_5K_5L_3M_2NO)$	$^4(SP_2D_3F_4G_4H_3I_3K_2LM)$	$^6(PFH)$		73
f^6, f^8	$^1(S_4PD_6F_4G_8H_4I_7K_3L_4M_2N_2Q)$	$^3(P_6D_5F_9G_7H_9I_6K_6L_3M_3NO)$	$^5(SPD_3F_2G_3H_2I_2KL)$	^7F	119
f^7	$^2(S_2P_5D_7F_{10}G_{10}H_9I_9K_7L_5M_4N_2OQ)$	$^4(S_2P_2D_6F_5G_7H_5I_5K_3L_3MN)$	$^6(PDFGHI)$	^8S	119

[a]H. N. Russell, Phys. Rev. 29, 782 (1927); R. C. Gibbs, D. T. Wilber, and H. E. White, Phys. Rev. 29, 790 (1927).

Rate Equations and Definitions

$$\frac{dN_{il}}{dt} = \sum_{jm} A_{iljm} N_{jm}$$

- N_{il} = Population per unit volume(cm^{-3}) of level *l* of ion species *i*
- A_{iljm} = Rate matrix(sec^{-1})
- Rate coefficients for processes which alter level populations, integrated atomic cross sections.
- These include electron collisions, photon collisions and spontaneous processes
- Depends on N_e, the number of free electrons per unit volume (cm^{-3}), for processes involving electron collisions, cross sections for the various processes, electron energy distribution, and radiation field.

*Another **T**heoretical **O**pacity **M**odeling **I**ntegrated **C**ode*

Atomic Physics Codes → **Atomic Models** → ***ATOMIC***

CATS:*Cowan Code*

RATS:*relativistic*

GIPPER:*ionization*

ACE:*e^- excitation*

http://aphysics2.lanl.gov/tempweb/

Los Alamos

fine structure

CFG-based

UTA's

energy levels

gf-values

e^- excitation

e^- ionization

$h\nu$-ionization

auto-ionization

LTE or NLTE

low or high-Z

spectral modeling

emission

absorption

power loss

Opacity Tables

Electron Energy Distribution Function(EEDF)

- Describes the distribution of free electrons as a function of electron energy. The fraction of electrons per unit energy interval. Unit is $(\text{energy})^{-1}$, usually eV.
- Described by the Maxwellian function for a given electron temperature kT_e(see below) for thermal plasmas.
$\int_0^\infty F(E)dE = 1$
- kT_e expressed in energy units, usually eV.
- $\mathrm{kT_e} = 11605\ ^\circ\mathrm{K}$

$$F(E) = \frac{2\sqrt{E}e^{-E/kT_e}}{\sqrt{\pi}(kT_e)^{3/2}}, \int_0^\infty F(E)dE = 1$$

Radiation field

- The number of photons per unit energy interval per unit volume between $h\nu$ and $h\nu + d\,h\nu$, units of $(\text{volume})^{-1}(\text{energy})^{-1}$, usually $\text{cm}^{-3}\text{eV}^{-1}$.
- kT_r in eV.
- For thermal plasmas the radiation field is given by the Planck function.

$$G(h\nu) = \frac{8\pi (h\nu)^2}{h^3 c^3 (e^{h\nu / kT_r} - 1)}$$

Electron and photon distributions at various temperatures

Maxwellian

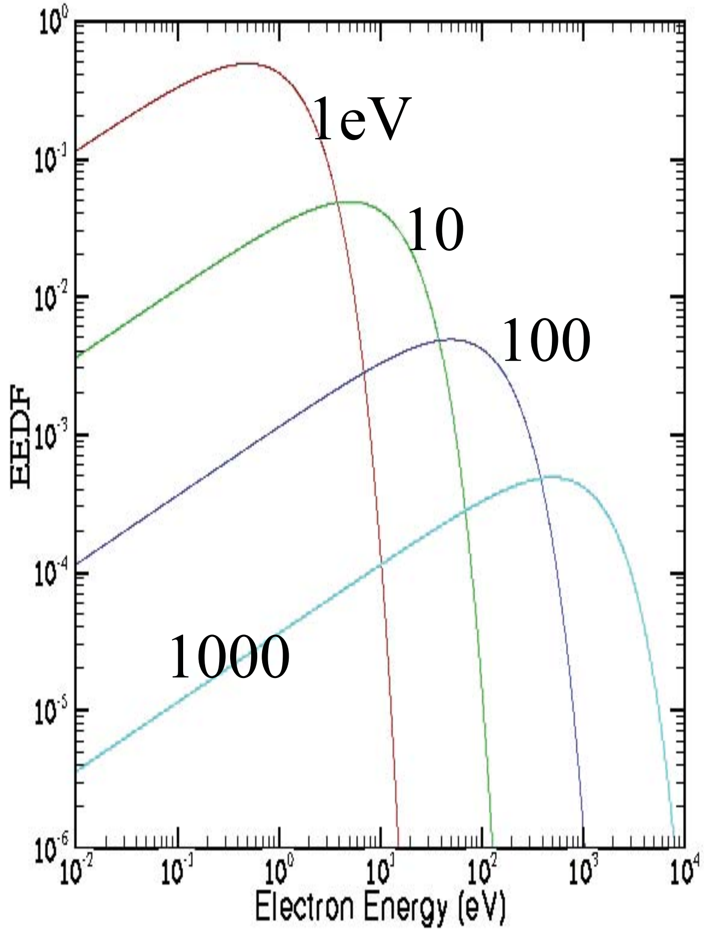

Planckian

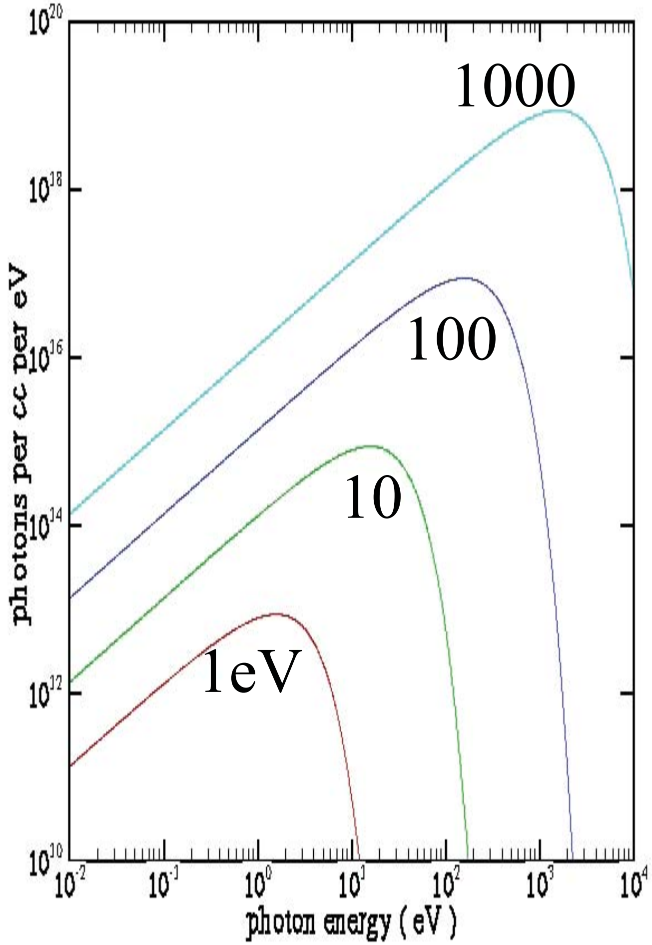

Atomic processes in plasmas induced by electrons and photons

excitation/de-excitation ionization/recombination

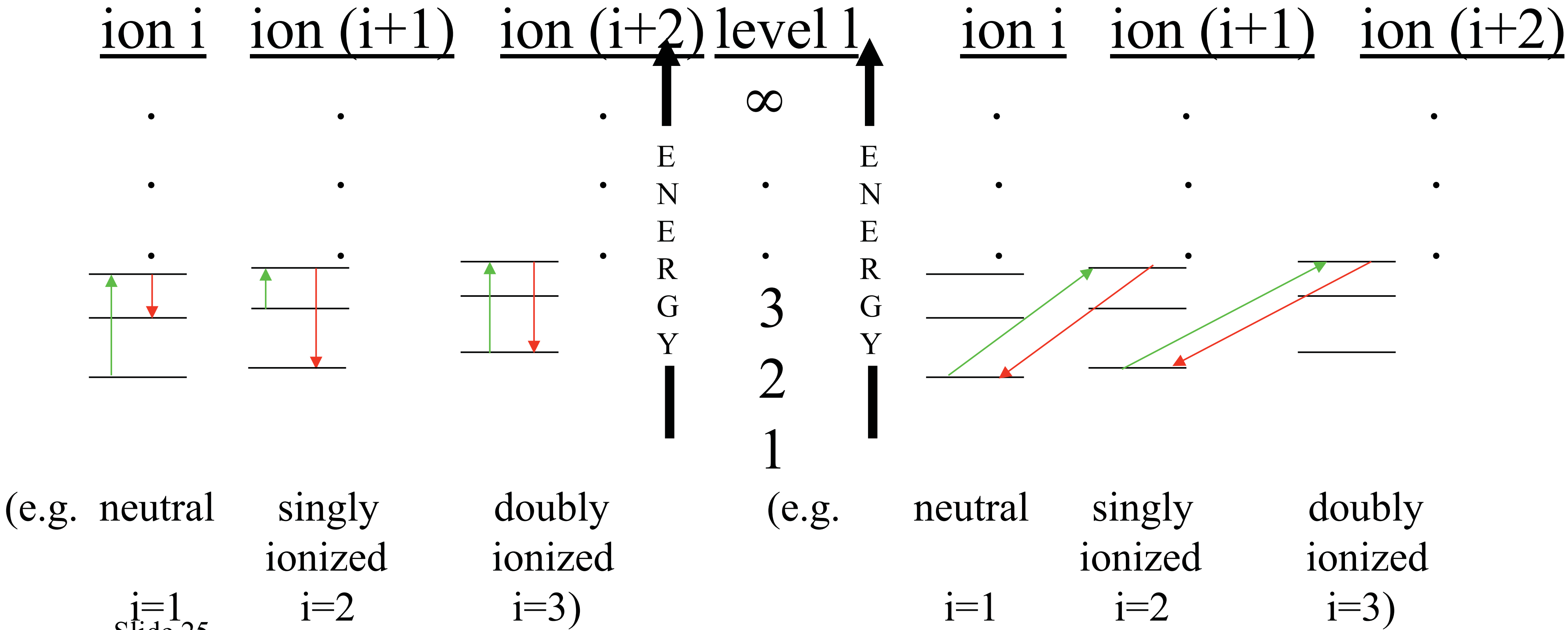

Processes

- Electron impact excitation/de-excitation:
  $e + A_{il} \Leftrightarrow e + A_{im}$
- Radiative excitation/spontaneous decay:
  $h\nu + A_{il} \Leftrightarrow A_{im}$
- Electron impact ionization / 3 body recombination:
  $e + A_{il} \Leftrightarrow A_{i+1m} + e + e$
- Photo-ionization / radiative recombination:
  $h\nu + A_{il} \Leftrightarrow A_{i+1m} + e$
- Auto-ionization / di-electronic capture:
  $A_{il}{}^{*} \Leftrightarrow A_{i+1m} + e$

Example: integrated rate coefficient

$$e^{-}(E) + A_{il} \leftrightarrow e^{-} + A_{im}(E')$$

$$E = E' + (E_{im} - E_{il}) = E' + E_0$$

number of excitations per volume per second between E *and* $E + dE$

$$= N_{il} N_e F(E) v(E) \sigma_{i \to m}(E) dE$$

the total number of excitation per volume per second is then

$$= N_{il} N_e s$$

where,

$$s = \int_{E_0}^{\infty} F(E) v(E) \sigma(E) dE = \text{rate coefficient}$$

LTE - Saha Equations

$$\frac{N_{i+1}N_e}{N_i} = \frac{Z_e Z_{i+1} e^{-\phi_i / kT}}{Z_i}$$

$$N_e = \sum_{il} q_i N_i$$

$$Z_i = \sum_i g_{il} e^{-E_{il} / kT}$$

$$Z_e = 2\left(\frac{2\pi m_e kT}{h^2}\right)^{3/2}$$

$$\frac{N_{il}}{N_i} = \frac{g_{il} e^{-E_{il} / kT}}{Z_i}$$

φ_i = ionization energy of ion *i*

q_i = charge of ion *i*

E_{il} = energy of level *l*

g_{il} = statisical weight of level *l*

N_i=population of ion *i*

N_e=electron density

N_{il}=population of level *l* ion *I*

Z_i,Z_e=partition functions

Principle of Detailed Balance

- Under LTE conditions the forward rate of each process is balanced by the inverse rate
- Therefore, the cross section for the inverse process may be derived from the cross section for the forward process
- This is required for the solution to approach the LTE limit

Detailed balance for excitation / de-excitation

$$e^{-}(E) + A_{il} \leftrightarrow e^{-} + A_{im}(E')$$

$$E = E' + (E_{im} - E_{il})$$

excitation rate = de - excitation rate at LTE

number of excitations per volume per second between

E *and* $E + dE$

$$N_{il} N_e F(E) v(E) \sigma_{i \to m}(E) dE = N_{im} N_e F(E') v(E') \sigma_{m \to i}'(E') dE'$$

Therefore σ' can be calculated from σ using LTE properties

relationships for N_{il}, N_e, $F(E)$, $v = \sqrt{2E / m_e}$

Derive an expression for the de - excitation cross section σ' in

terms of the excitation cross section σ.

Coronal Equilibrium

$$\frac{dN_i}{dt} = I_{i-1}N_{i-1} - (R_i + I_i)N_i + R_{i+1}N_{i+1} = 0$$

- I_i=net ionization rate coefficient from from ground state of ion i including inner shell excitation/autoinization
- R_{i}=net recombination rate from ground state of ion i including recombination into excited states of ion i-1
- Low density limit
- Solar corona model
- Only ground states significantly populated
- Radiative decay rates >> e^- impact excitation rates

Solution of Rate Equations

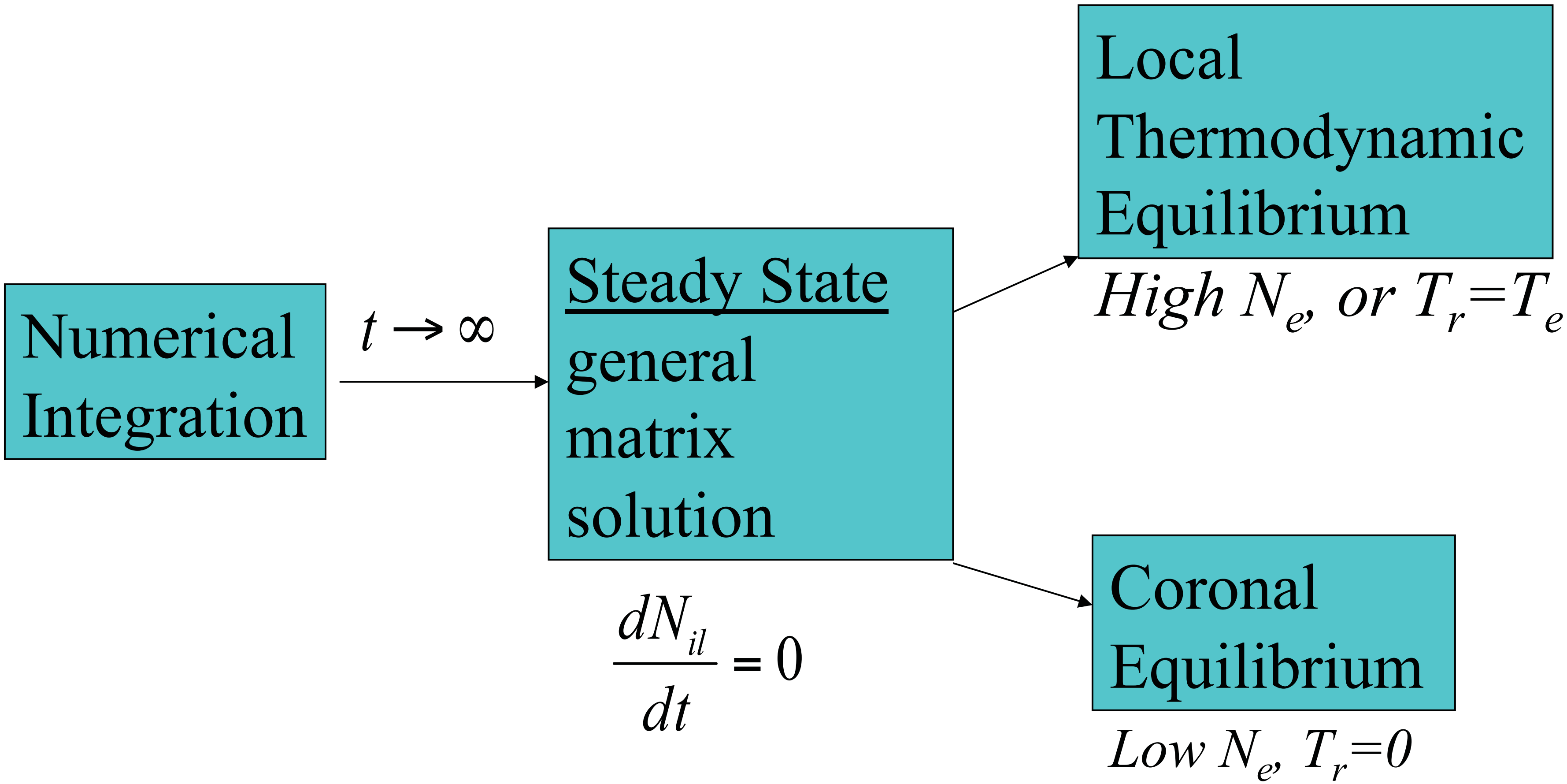

e^- Impact Excitation ↔ De-Excitation

$$e^-(E) + A_{il} \leftrightarrow e^-(E') + A_{im}$$

$$E' = E - E_0$$

$$E_0 = E_{im} - E_{il}$$

$$\frac{dN_{il}}{dt} = -sN_e N_{il} + tN_e N_{im}$$

$$s = \int_{E_0}^{\infty} F(E, kT_e) v(E) \sigma(E) dE$$

$$t = \frac{g_{il}}{g_{im}} e^{E_0/kT_e} s,$$

s and t in cm^3 / sec

E = impact energy

E' = final energy

E_0 = threshold energy

N_{il} = state population

N_e = electron density

T_e = electron temperature

s = excitation rate coefficient

t = de-excitation rate coefficient

Ex : $e^- + 1s^2 \leftrightarrow e^- + 1s2p$

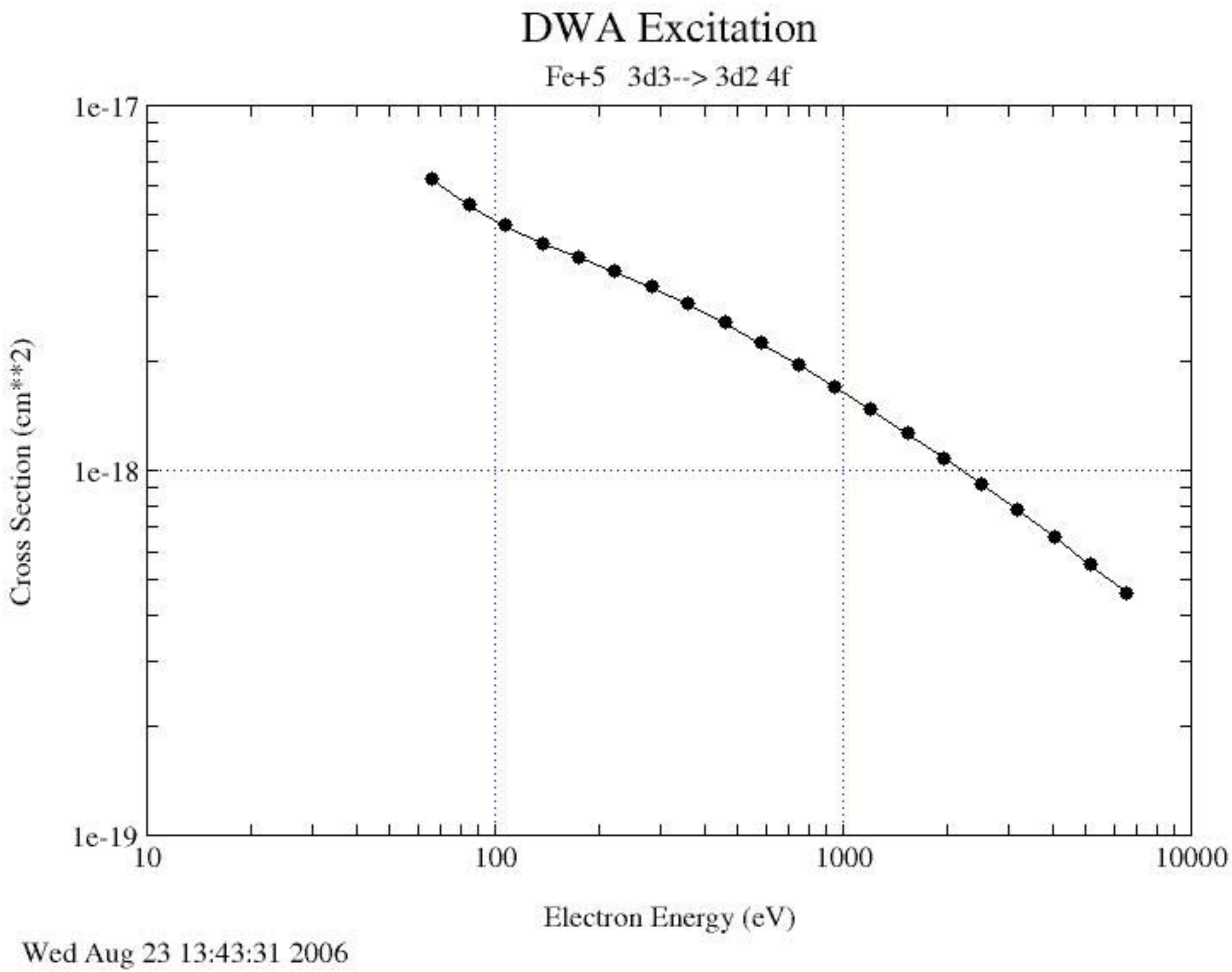
DWA Excitation
Fe+5 3d3--> 3d2 4f
1e-17
1e-18
1e-19
10
100
1000
10000
Cross Section (cm**2)
Electron Energy (eV)
Wed Aug 23 13:43:31 2006

Photo-Excitation ↔ Decay

$$h\nu + A_{il} \leftrightarrow A_{im}$$

$$h\nu_0 = E_{im} - E_{il}$$

$$\frac{dN_{il}}{dt} = -uN_{il} + yN_{im} + zN_{im}$$

$$u = \frac{he^2\pi}{m_e}\frac{(gf)_{ilm}}{g_{il}}G(h\nu_0, kT_r)$$

$$y = \frac{8\pi^2 e^2}{h^2 c^3 m_e}\frac{(gf)ilm}{g_{im}}(h\nu_0)^2$$

$$y = 4.338\times 10^7 \frac{(gf)ilm}{g_{im}}(h\nu_0)^2$$

$$z = \frac{(gf)ilm}{g_{im}}u$$

u,y,z *in* $\sec^{-1}$ $, h\nu_0$ *in* eV

$h\nu$ = photon energy

$h\nu_0$ = transition energy

N_{il} = state population

kT_r = radiation temperature

u = excitation rate coefficient

y = spontaneous decay rate coefficient (Einstein A coefficient)

z = stimulated decay rate coefficient

$u = z = 0$ with no radiation field

Ex : $h\nu + 1s^2 \leftrightarrow 1s^1 2p^1$

Fe^{+5}: $3d^3$-$3d^24f$

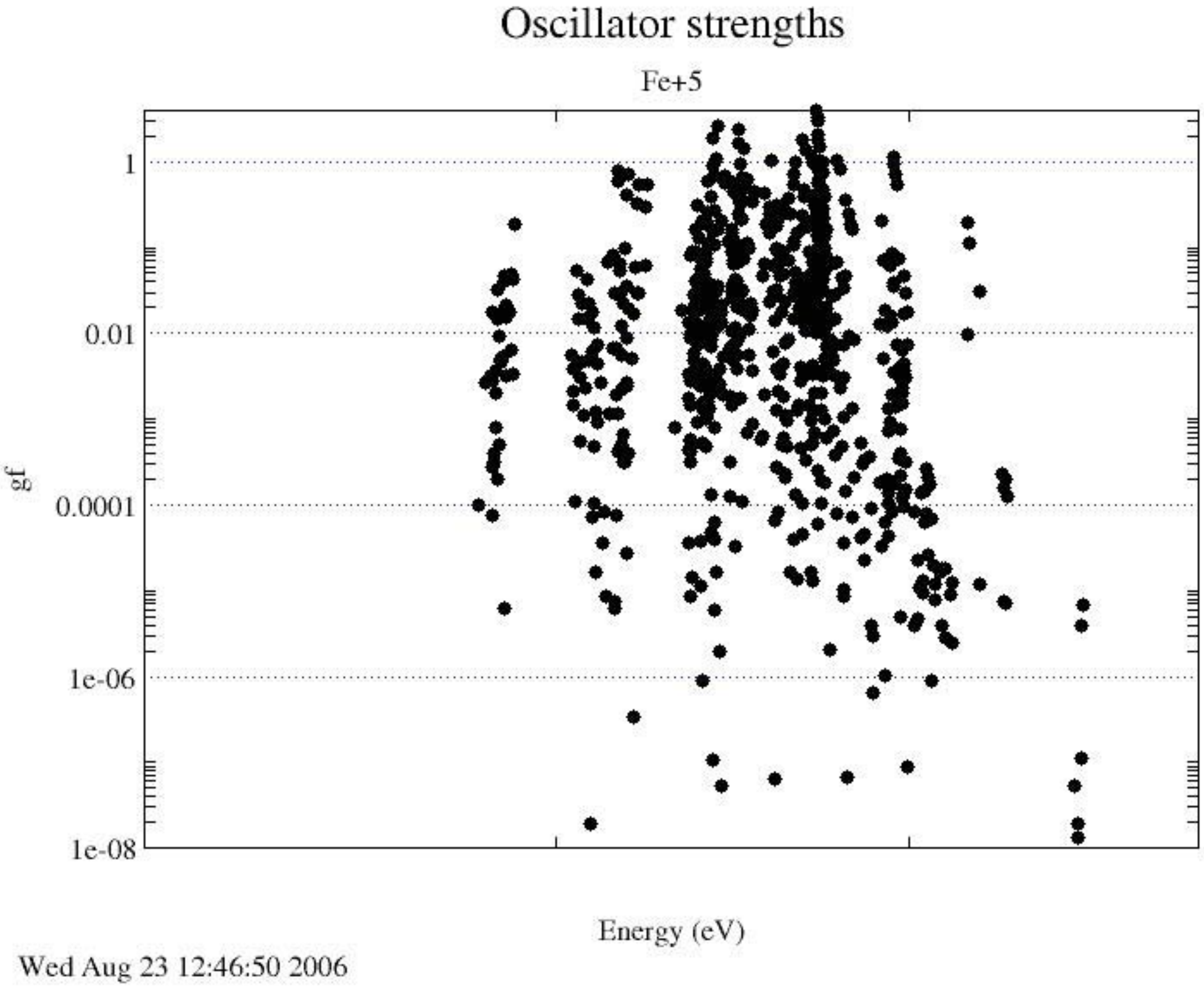

Photo-Ionization ↔ Radiative Recombination

$$h\nu + A_{il} \leftrightarrow e^{-}(E) + A_{jm}$$

$$h\nu = E_{jm} - E_{il} + E = h\nu_0 + E$$

$$\frac{dN_{il}}{dt} = -pN_{il} + rN_e N_{jm} + qN_e N_{jm}$$

$$p = \int_{h\nu_0}^{\infty} G(h\nu, kT_r)\sigma_{iljm}(h\nu)cdh\nu$$

$$r = \frac{g_{il}}{g_{jm}} \frac{1}{2^{1/2} m_e^{3/2} c^2} \int_0^{\infty} F(E, kT_e) \frac{(h\nu_0 + E)^2}{E^{1/2}} \sigma_{iljm}(h\nu_0 + E)dE$$

$$r + q = 1.66 \times 10^{-22} \frac{g_{il}}{g_{jm}} \frac{e^{h\nu_0/kT}}{kT^{3/2}} p$$

p is $\sec^{-1}$, r, q, in $cm^3/\sec$, kT, E, $h\nu_0$ in eV.

$h\nu$ = photon energy

$h\nu_0$ = ionization energy

u = photoionization rate coefficient

r = radiative recombination rate coefficient

$r + q$ = radiative recombination rate coefficient with stimulated emission, $kT_e = kT_r$

$q = 0$ with no radiation field

Ex : $h\nu + 1s^2 \leftrightarrow 1s^1 + e^-$

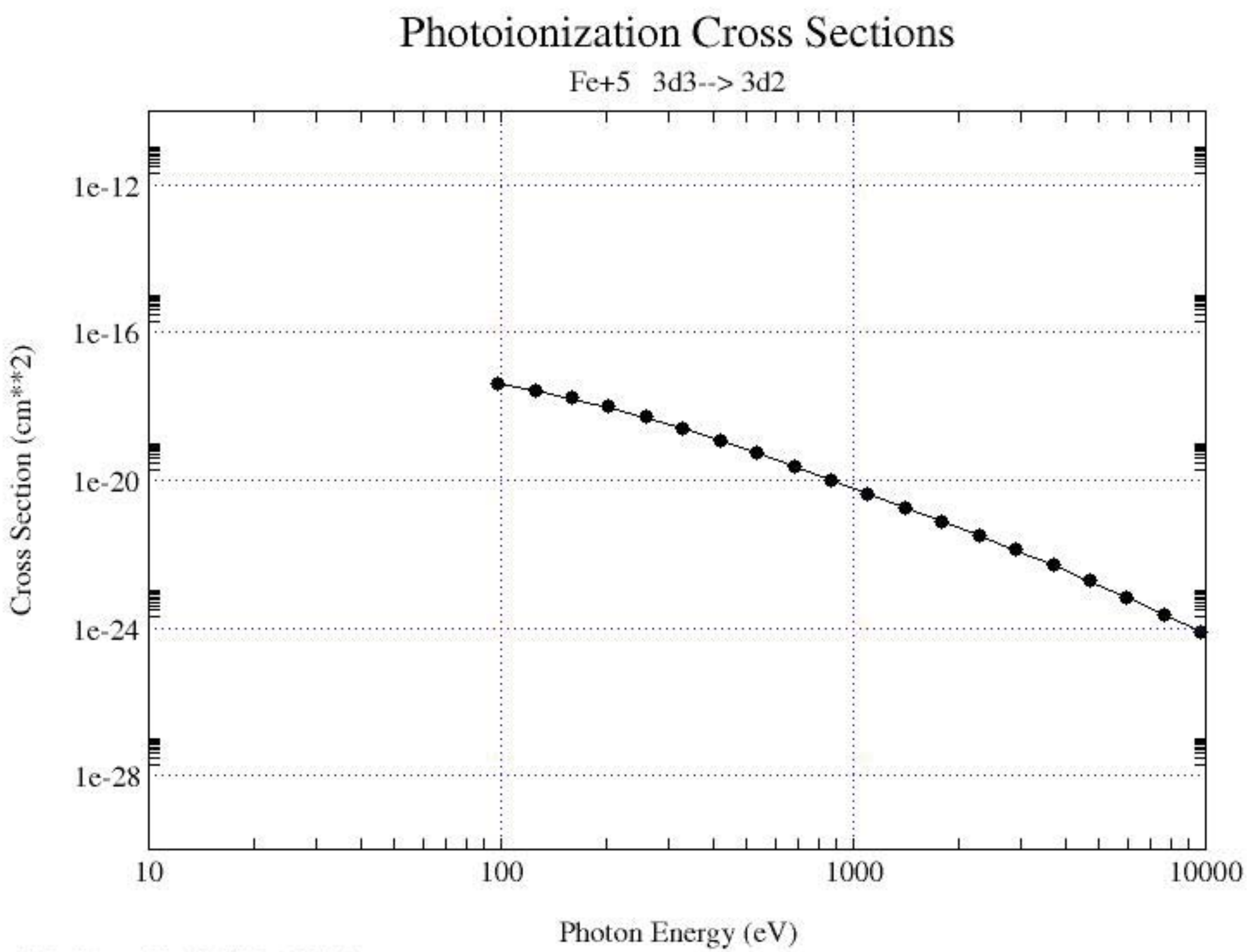

Wed Aug 23 13:52:24 2006

e^- Impact Ionization ↔ Three-Body Recombination

$$e^-(E) + A_{il} \leftrightarrow e^-(E') + e^-(E'') + A_{jm}$$

$$E = E_{jm} - E_{il} + E' + E'' = E_0 + E' + E''$$

$$\frac{dN_{il}}{dt} = -cN_e N_{il} + bN_e^2 N_{jm}$$

$$c = \int_{E_0}^{\infty} F(E, kT_e) v(E) Q(E) dE$$

$$b = 1.66 \times 10^{-22} \frac{g_{il}}{g_{jm}} \frac{e^{E_0/kT_e}}{(kT_e)^{3/2}} c$$

c in $\mathrm{cm}^3/\mathrm{sec}$, b in $\mathrm{cm}^6/\mathrm{sec}$

kT_e and E_0 in eV

$E = e$ impact energy.

E_0 = ionization energy.

c = e^- impact ionization rate coefficient.

b = three - body recombination rate coefficient, Maxwellian only.

Q = e^- impact ionization cross section.

Ex : $1s^2 + e^- \leftrightarrow 1s^1 + e^- + e^-$

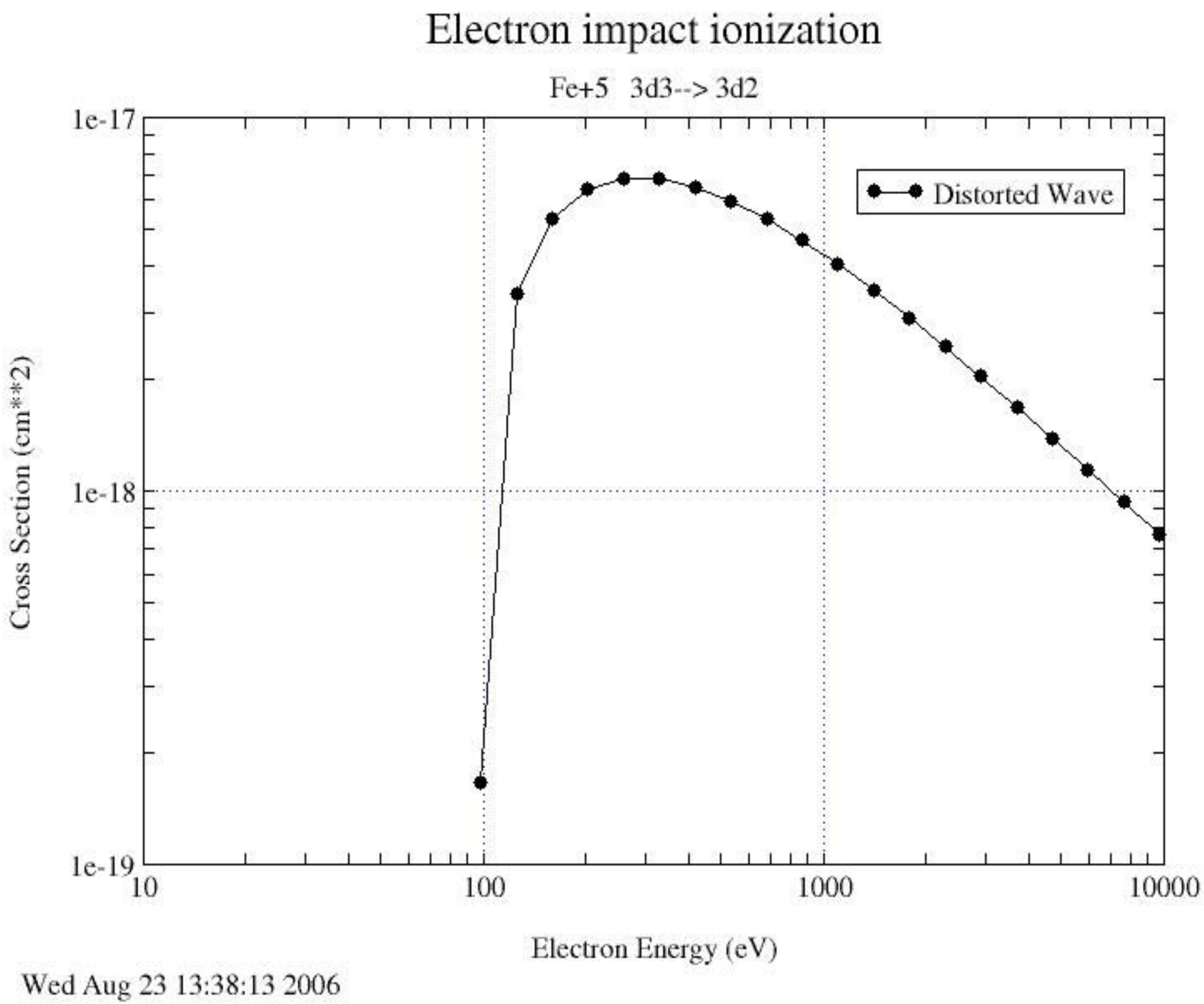

Electron impact ionization
Fe+5 3d3--> 3d2
1e-17
1e-18
1e-19
Cross Section (cm**2)
Distorted Wave
10
100
1000
10000
Electron Energy (eV)
Wed Aug 23 13:38:13 2006

Auto-Ionization ↔ Di-Electronic Capture

$$A_{il} \leftrightarrow e^{-}(E_0) + A_{jm}$$

$$E_0 = E_{jm} - E_{il}$$

$$\frac{dN_{il}}{dt} = -aN_{il} + dN_e N_{jm}$$

$$a = A^{a}_{iljm}$$

$$d = 1.66 \times 10^{-22} \frac{g_{il}}{g_{jm}} \frac{e^{-E_0/kT_e}}{(kT_e)^{3/2}} a$$

a in sec^{-1} and d in cm^{3} / sec

E_0 and kT_e in eV

E_0 = ionization energy.

a = auto - ionization rate.

d = di - electronic capture rate coefficient, Maxwellian only.

Ex : He - like $2s^2 \leftrightarrow 2s^1 + e^-$

Fe^{+5}:$3d^1 4f^2$-$3d^2$

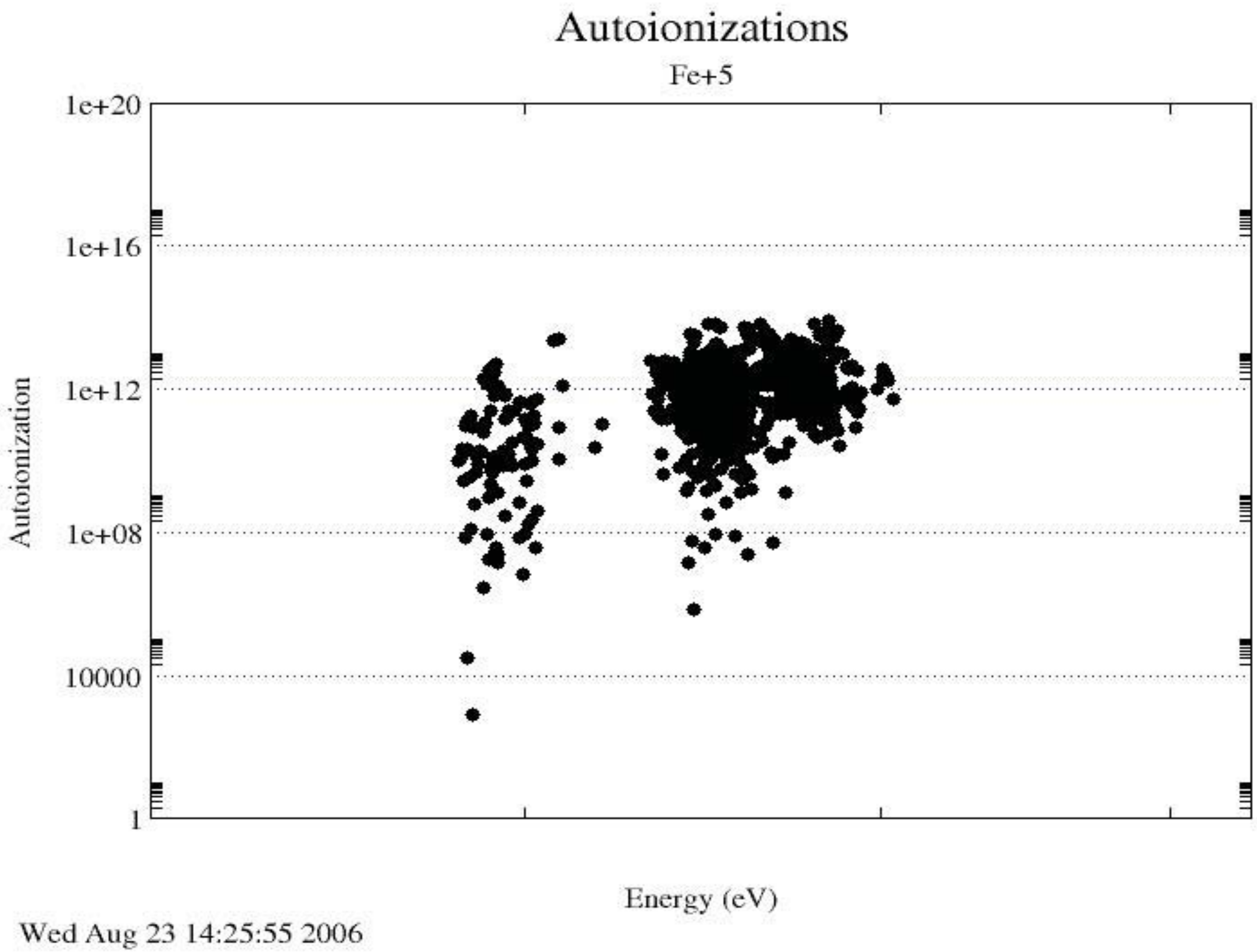

Emission spectra

- **Line or bound-bound** contribution:
- The number of emitting photons per second per volume per unit energy interval per transition:

$$N_{im}\frac{8\pi^2 e^2}{h^2 c^3 m_e}\frac{(gf)_{ilm}}{g_{im}}(h\nu_0)^2\Phi_{ilm}(h\nu)$$

$$h\nu_0 = E_{im} - E_{il}$$

$$\Phi_{ilm}(h\nu) = \text{line shape}$$

$$\int_0^\infty \Phi_{ilm}(h\nu)dh\nu = 1$$

$$\text{e.g.}\,\Phi = \frac{w/\pi}{(h\nu - h\nu_0)^2 + w^2}\ \text{or}$$

$$\Phi = \sqrt{\ln 2/(\pi w^2)}\,e^{-\ln 2(h\nu - h\nu_0)^2/w^2}$$

$$w = HWHM$$

Emission spectra, lines, cont.

- The total amount radiated energy per second per volume per unit energy interval, sum over all transitions:

$$\sum N_{im} \frac{8\pi^2 e^2}{h^2 c^3 m_e} \frac{(gf)ilm}{g_{im}} (h\nu_0)^3 \Phi_{ilm}(h\nu)$$

Emission spectra

- **Recombination or free-bound continuous** contribution
- The total amount radiated energy per second per volume per unit energy interval, sum over all transitions:

$$\sum N_{jm} N_e \frac{g_{il}}{g_{jm}} \frac{1}{2^{1/2} m_e^{3/2} c^2} F(E, kT_e) \frac{(h\nu)^3}{E^{1/2}} \sigma_{iljm}(h\nu)$$

$$h\nu = E_{jm} - E_{il} + E = h\nu_0 + E$$

Emission spectra

- **free-free or Bremsstralung continuous contribution**
- **free electron decelerates in plasma and emits a photon**
- **simple hydrogenic formula**
- **The total amount radiated energy per second per volume per unit energy interval, sum over all transitions:**

$$9.585552\times10^{-14}\,\frac{N_e e^{-h\nu/kT_e}}{(kT_e)^{1/2}}\sum N_i q_i^2$$

$$N_i = \text{population of ion i}$$

$$q_i = \text{charge of ion i}$$

Power Loss Is Obtained by Integrating Emission Over ALL Photon Energies

$$P_{tot} = P_{bb} + P_{bf} + P_{ff}$$

$$P_{bb} = \sum_{im} N_{im}(y_{ilm} + z_{ilm})(E_{im} - E_{il})$$

$$P_{bf} = \sum_{im} N_{jm} N_e (r_{iljm} + q_{iljm})(E_{jm} - E_{il} + (3/2)kT_e)$$

$$P_{ff} = 9.55 \times 10^{-14} (kT_e)^{1/2} N_e \sum_i q_i^2 N_i$$

P in $eV/(sec\ cm^3)$, $1J = 6.24 x 10^{18} eV$, $1W = 1J/sec$

Multi-Element Kinetics Algorithm*

- **Specify:** $N_a^{(1)}, N_a^{(2)}, \ldots, N_a^{(N)}$ and δN_e
- **Initialize:** $Guess - \; {}^{(0)}N_e$
- **For** $i \geqq 0$ **:** Solve the set of rate equations to obtain the $\overline{Z}^{(s)}$ for each species,

$$\begin{aligned} {}^{(i)}N_e; kT &\rightarrow {}^{(i)}\overline{Z}^{(1)} \\ {}^{(i)}N_e; kT &\rightarrow {}^{(i)}\overline{Z}^{(2)} \\ &\vdots \\ {}^{(i)}N_e; kT &\rightarrow {}^{(i)}\overline{Z}^{(N)} \end{aligned} \tag{1}$$

$${}^{(i)}\overline{Z}^{(1)}N_a^{(1)} +{}^{(i)} \overline{Z}^{(2)}N_a^{(2)} + \cdots +{}^{(i)} \overline{Z}^{(N)}N_a^{(N)} ={}^{(i+1)} N_e \tag{2}$$

if ${}^{(i+1)}N_e \leqq{}^{(i)} N_e + \delta N_e$ **then**
Multi-element calc. converged!
EXIT For Loop
else
Increment $i : i = i + 1$
Return to begining of For Loop
end if

- **End For Loop**

** M.E. Sherrill et al, Phys. Rev. E **76** 05640 (2007)*

Solar Corona Calculations

- Atomic structure and collisional data were computed for all ion stages of the 15 most abundant solar coronal elements:

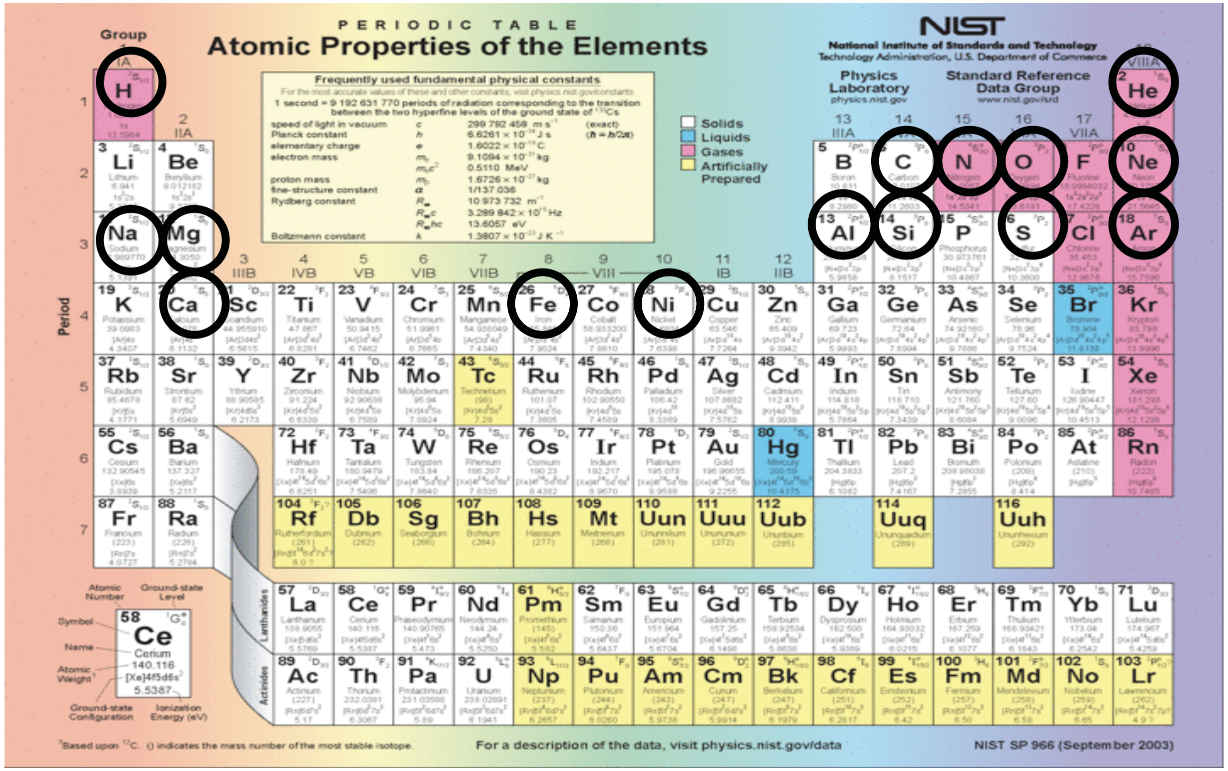

- Collisional data was computed using ***PWB*** and ***FOMBT/DW*** approaches, to test the sensitivity of the radiative losses to the quality of the excitation data.

Ion balance is calculated consistently with power loss

It is also instructive to know which ion stages contribute most to the radiative losses.

For C, at the temperatures at which it is the strongest contributor, we find that most of the emission arises from **C IV** and **C V** ions.

For O, **O V**, **O VI**, and **O VII** contribute most at the temperatures for which O dominates.

We also see that many ion stages of **Si** and **Fe** are present for a wide temperature range and so must be included.

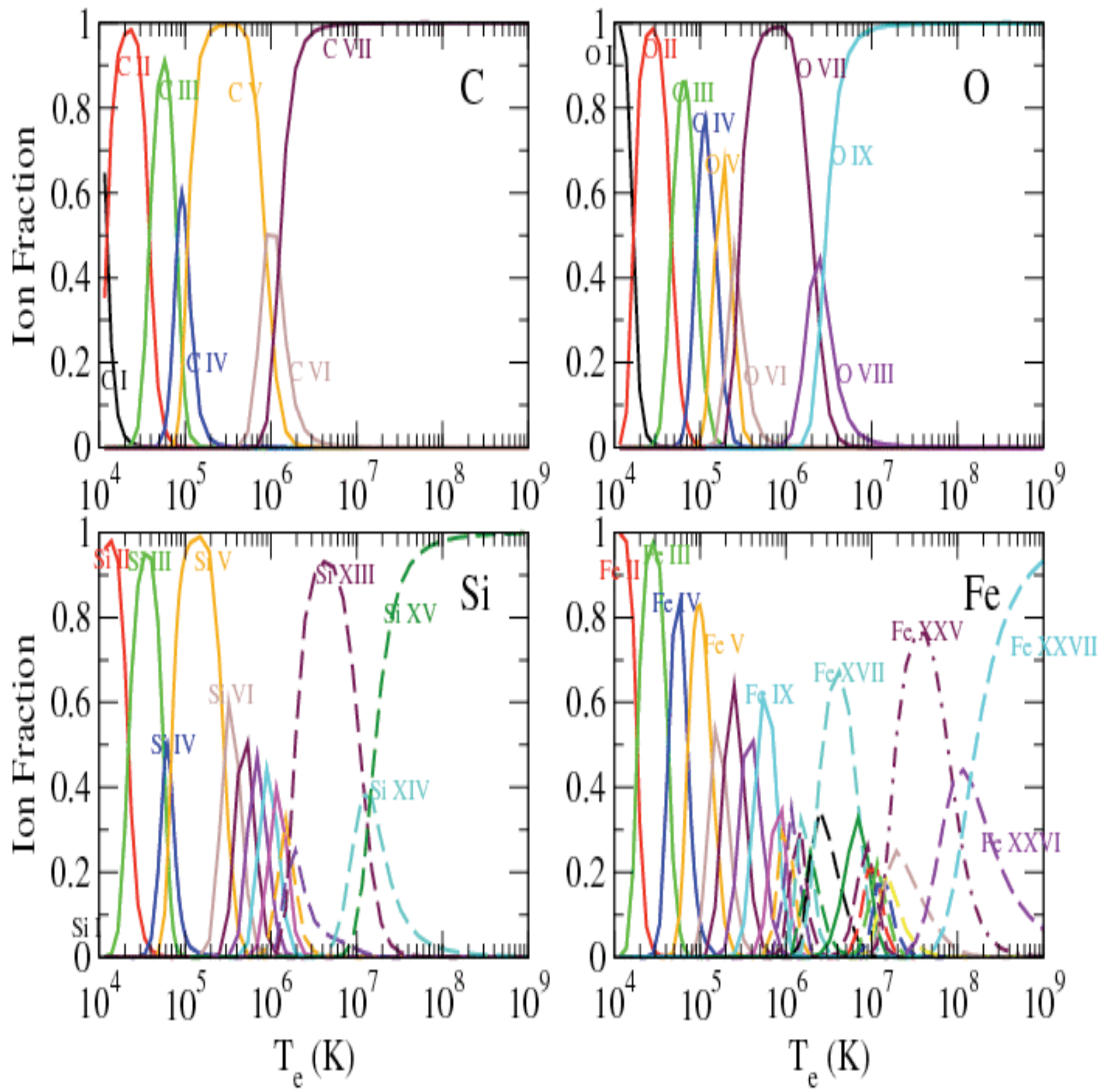

Results – comparisons to previous work

We compare the ATOMIC calculations to previous work of Landi & Landini (1999) and from the CHIANTI database

Substantial differences are found with Landi & Landini (1999) over most of the temperature range

Significant differences with the latest CHIANTI calculations persist at low temperatures below 10^6 K (~ 100 eV)

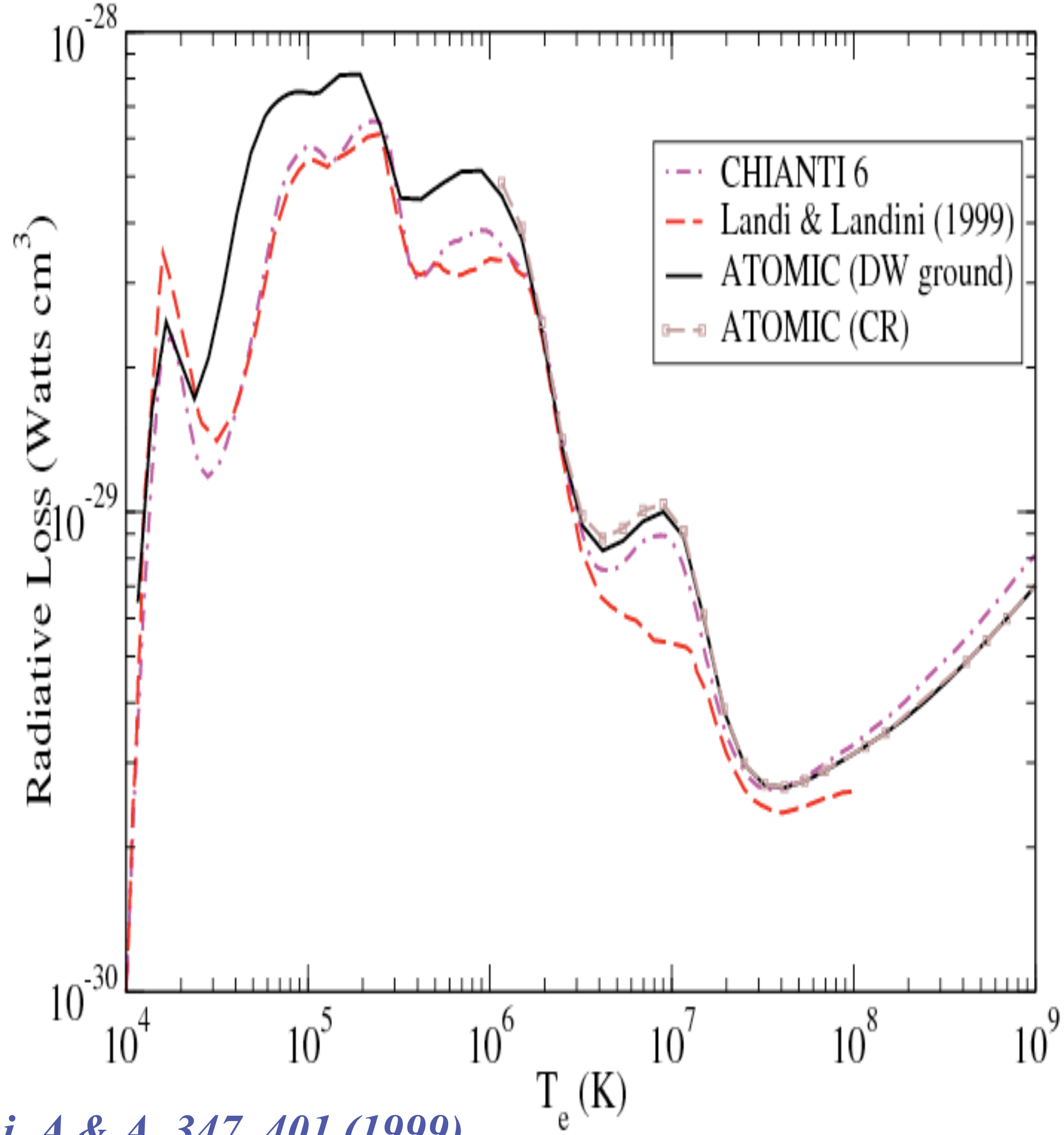

Landi & Landini, A & A, 347, 401 (1999).

Radiative losses from the individual elements

We present the contribution of the radiative losses from the individual 15 elements included in our calculation

At low temperatures **H**, **He**, **C**, and **O** are the dominant contributors

At high temperatures, **Si**, and **Fe** contribute most to the radiative loss, although at the highest temperatures, continuum radiation from **H** also contributes strongly

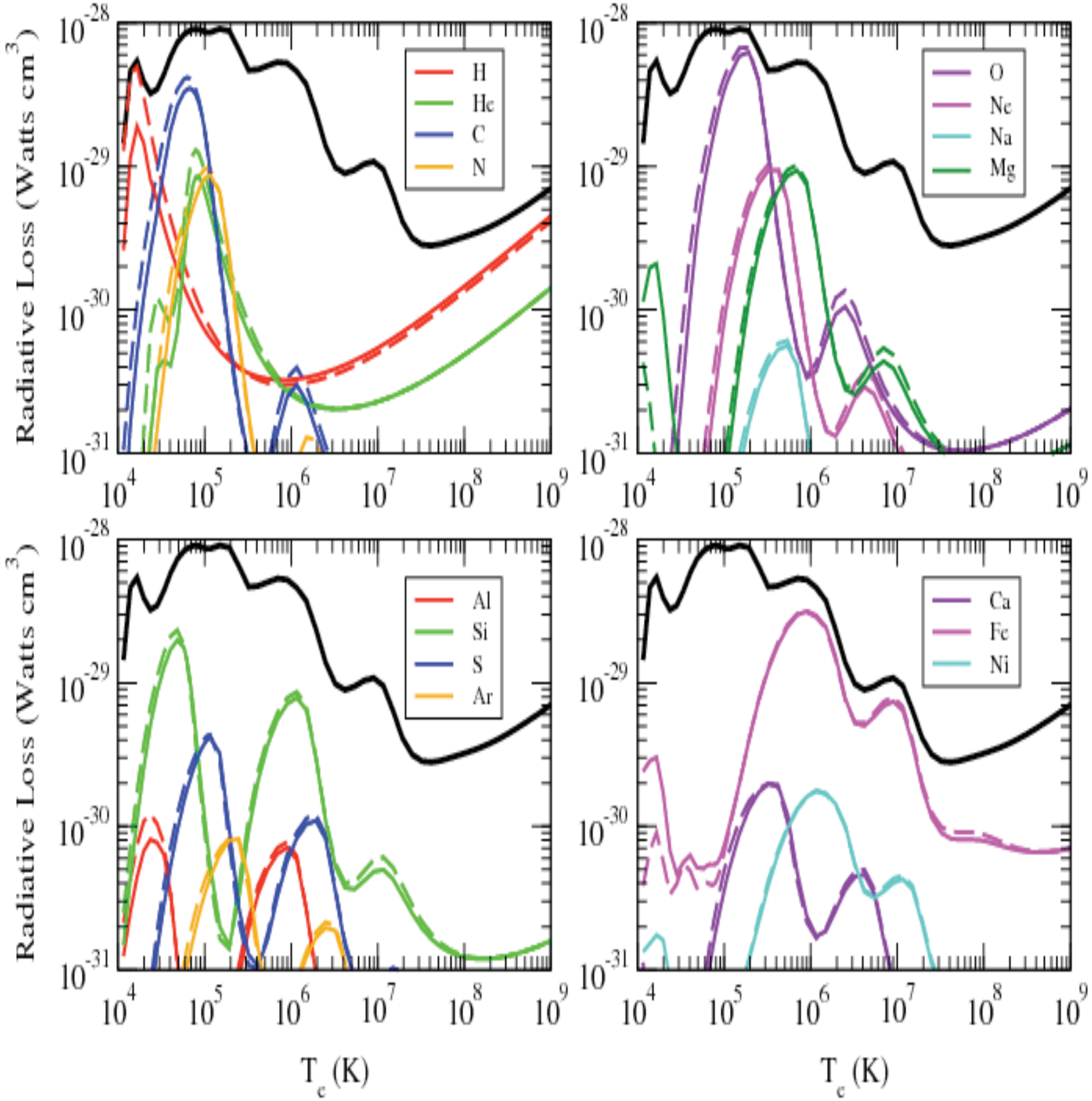

Colgan et al, Astrophysical Journal, accepted (2008).

Sensitivity to elemental abundances

The previous radiative losses were computed using "quiet region" elemental abundances

Some regions of the corona have different abundances of elements with low (< 10 eV) first-ionization-potentials (FIPs)

These include the elements Na, Mg, Al. Si, Ca, Fe, and Ni

Thus we present the radiative losses for a variety of FIP bias values (relative to the photospheric abundances)

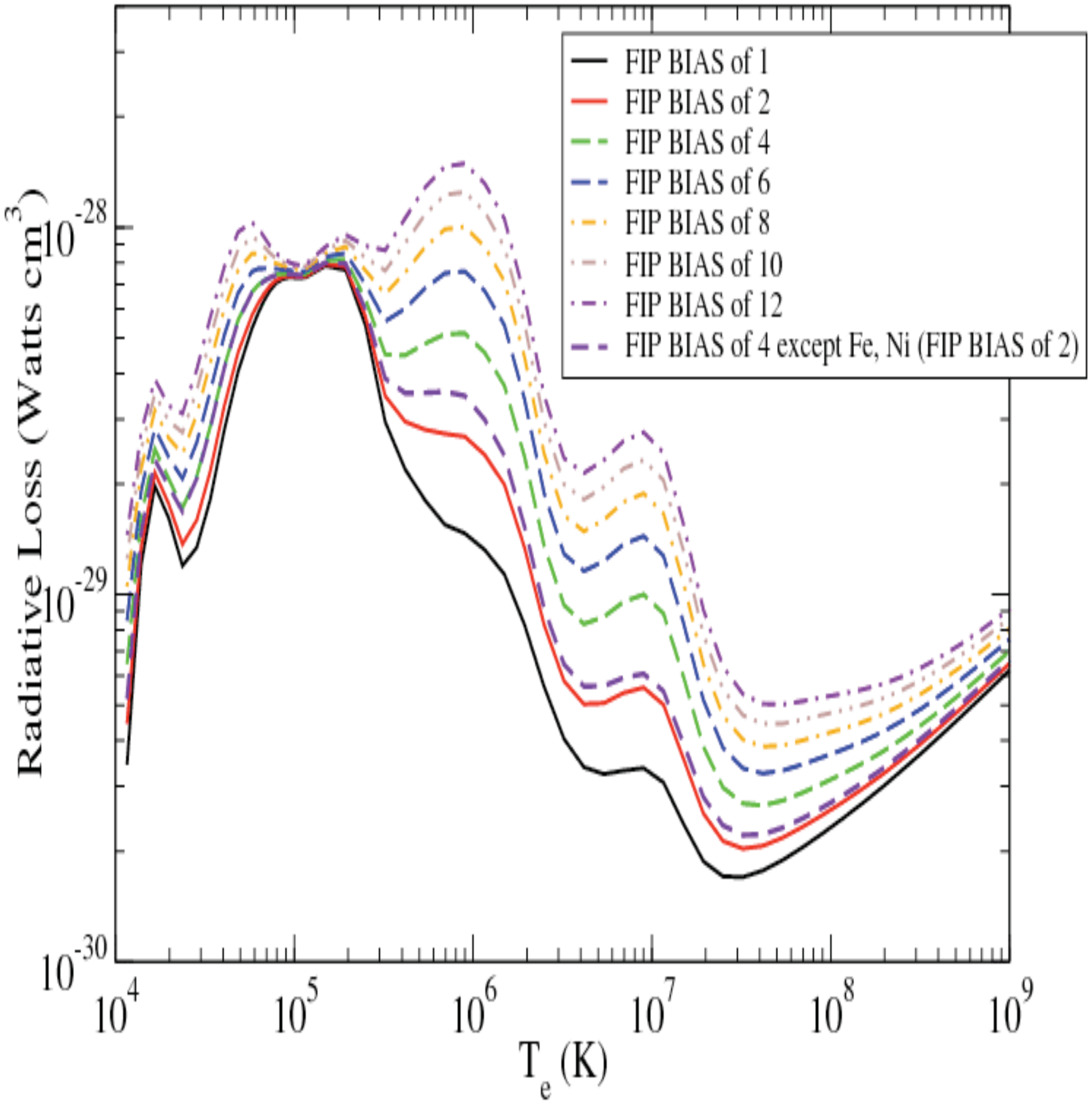

Multi-Element Kinetics Algorithm*

- **Specify:** $N_a^{(1)}, N_a^{(2)}, \ldots, N_a^{(N)}$ and δN_e
- **Initialize:** $Guess -\ \ {}^{(0)}N_e$
- **For** $i \geqq 0:$ Solve the set of rate equations to obtain the $\overline{Z}^{(s)}$ for each species,

$$\begin{aligned} {}^{(i)}N_e; kT &\rightarrow {}^{(i)}\overline{Z}^{(1)} \\ {}^{(i)}N_e; kT &\rightarrow {}^{(i)}\overline{Z}^{(2)} \\ &\vdots \\ {}^{(i)}N_e; kT &\rightarrow {}^{(i)}\overline{Z}^{(N)} \end{aligned} \tag{1}$$

$${}^{(i)}\overline{Z}^{(1)}N_a^{(1)} + {}^{(i)}\overline{Z}^{(2)}N_a^{(2)} + \cdots + {}^{(i)}\overline{Z}^{(N)}N_a^{(N)} = {}^{(i+1)}N_e \tag{2}$$

if ${}^{(i+1)}N_e \leqq {}^{(i)}N_e + \delta N_e$ **then**
Multi-element calc. converged!
EXIT For Loop
else
Increment $i : i = i + 1$
Return to begining of For Loop
end if

- **End For Loop**

** M.E. Sherrill et al, Phys. Rev. E **76** 05640 (2007)*

Solar Corona Calculations

- Atomic structure and collisional data were computed for all ion stages of the 15 most abundant solar coronal elements:

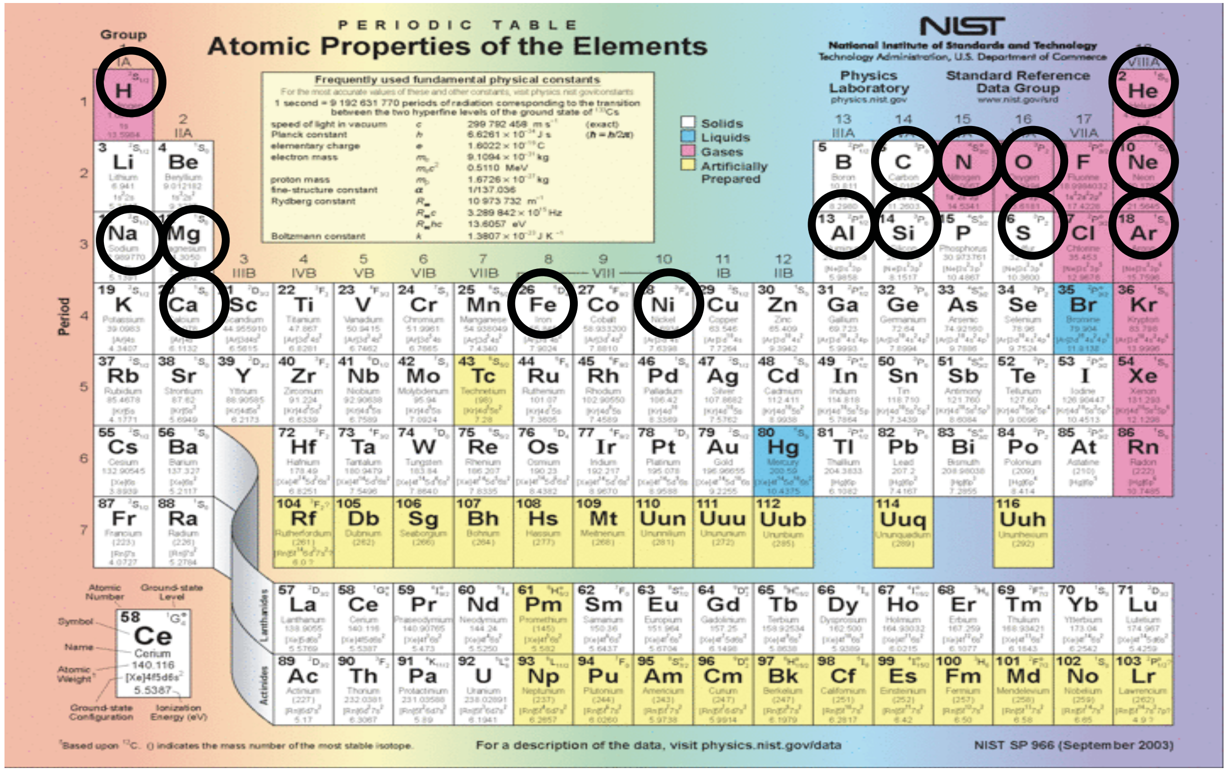

- Collisional data was computed using ***PWB*** and ***FOMBT/DW*** approaches, to test the sensitivity of the radiative losses to the quality of the excitation data.

Ion balance is calculated consistently with power loss

It is also instructive to know which ion stages contribute most to the radiative losses.

For C, at the temperatures at which it is the strongest contributor, we find that most of the emission arises from **C IV** and **C V** ions.

For O, **O V**, **O VI**, and **O VII** contribute most at the temperatures for which O dominates.

We also see that many ion stages of **Si** and **Fe** are present for a wide temperature range and so must be included.

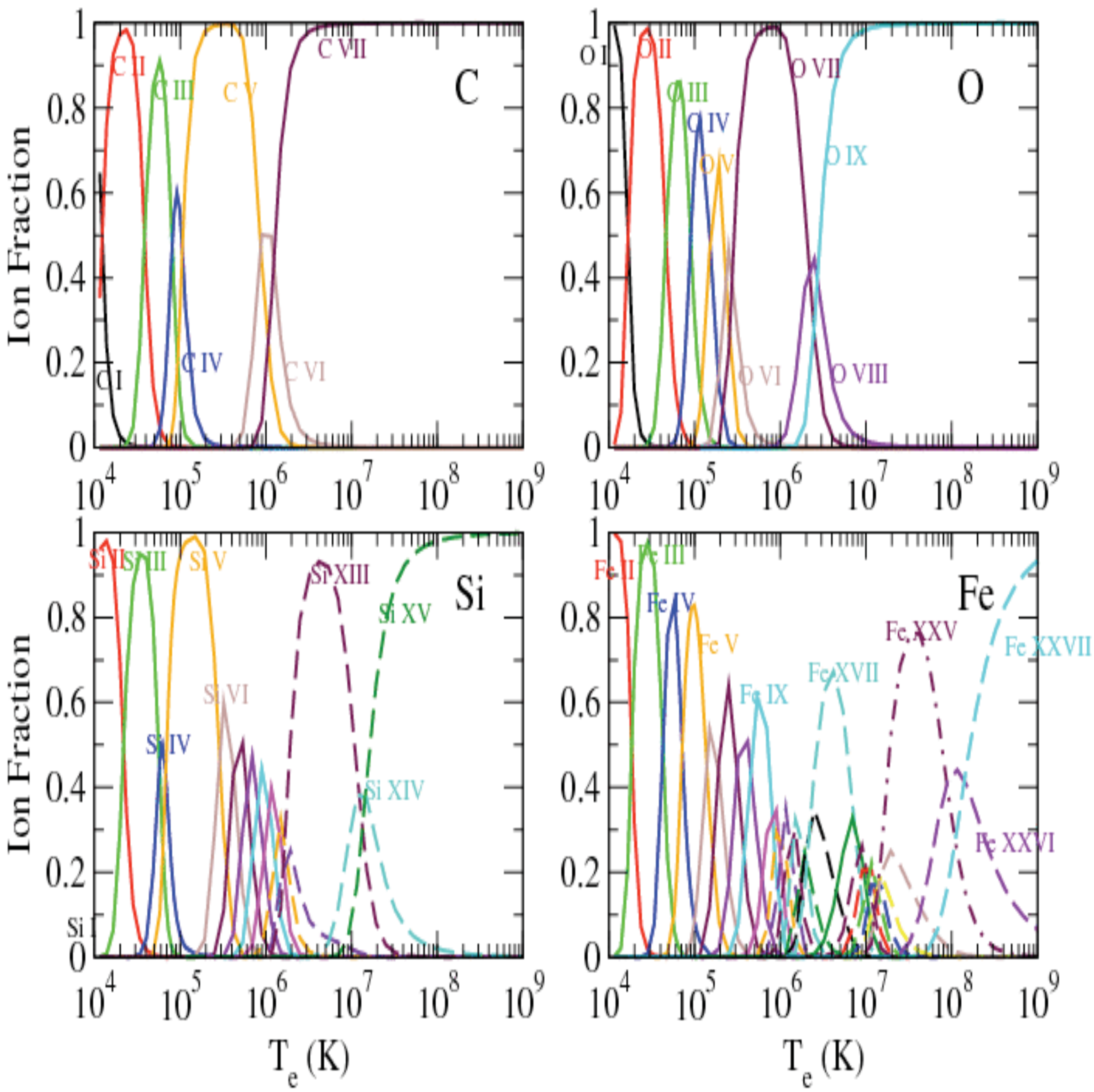

Results – comparisons to previous work

We compare the ATOMIC calculations to previous work of Landi & Landini (1999) and from the CHIANTI database

Substantial differences are found with Landi & Landini (1999) over most of the temperature range

Significant differences with the latest CHIANTI calculations persist at low temperatures below 10^6 K (~ 100 eV)

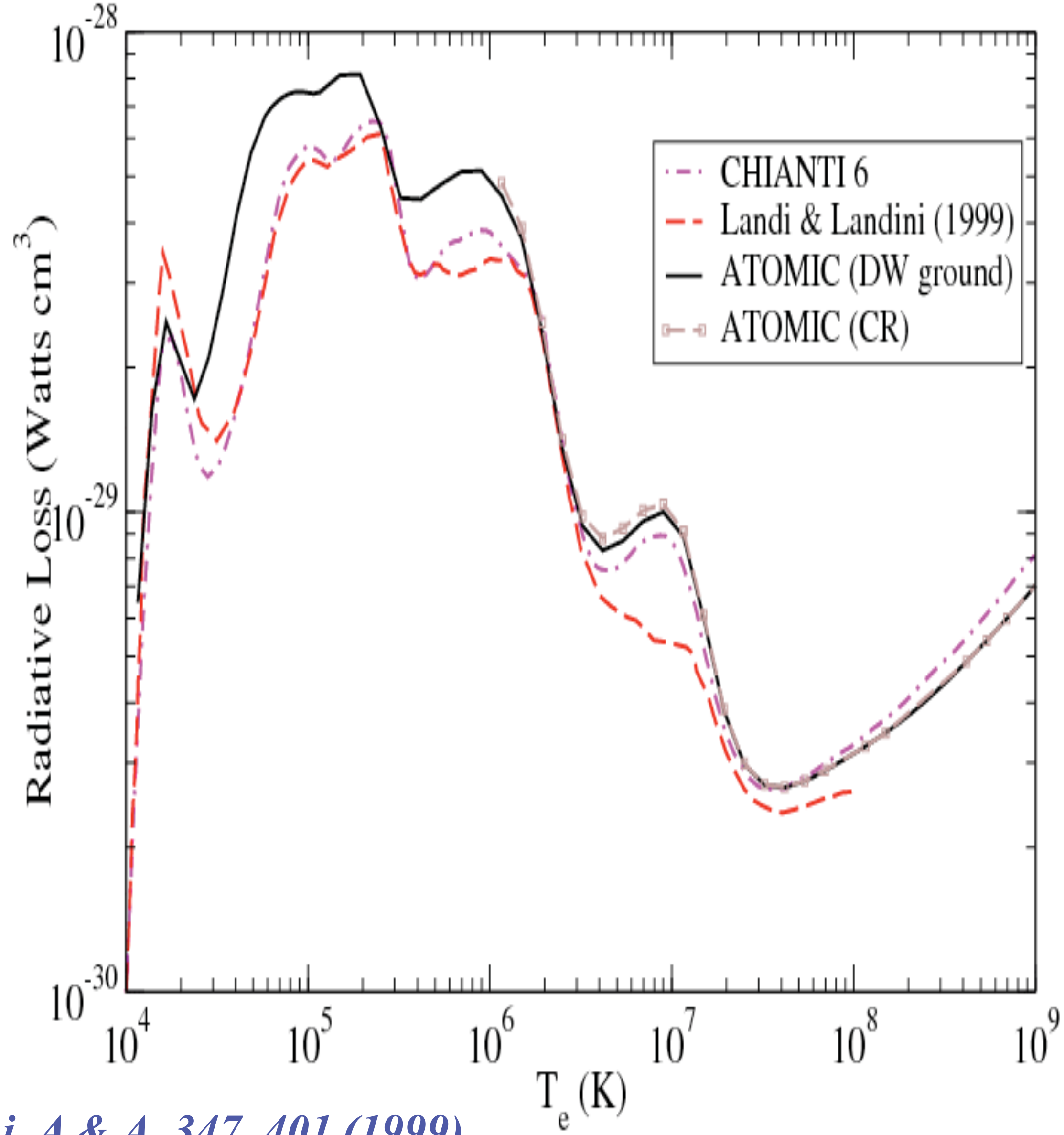

Landi & Landini, A & A, 347, 401 (1999).

Radiative losses from the individual elements

We present the contribution of the radiative losses from the individual 15 elements included in our calculation

At low temperatures **H**, **He**, **C**, and **O** are the dominant contributors

At high temperatures, **Si**, and **Fe** contribute most to the radiative loss, although at the highest temperatures, continuum radiation from **H** also contributes strongly

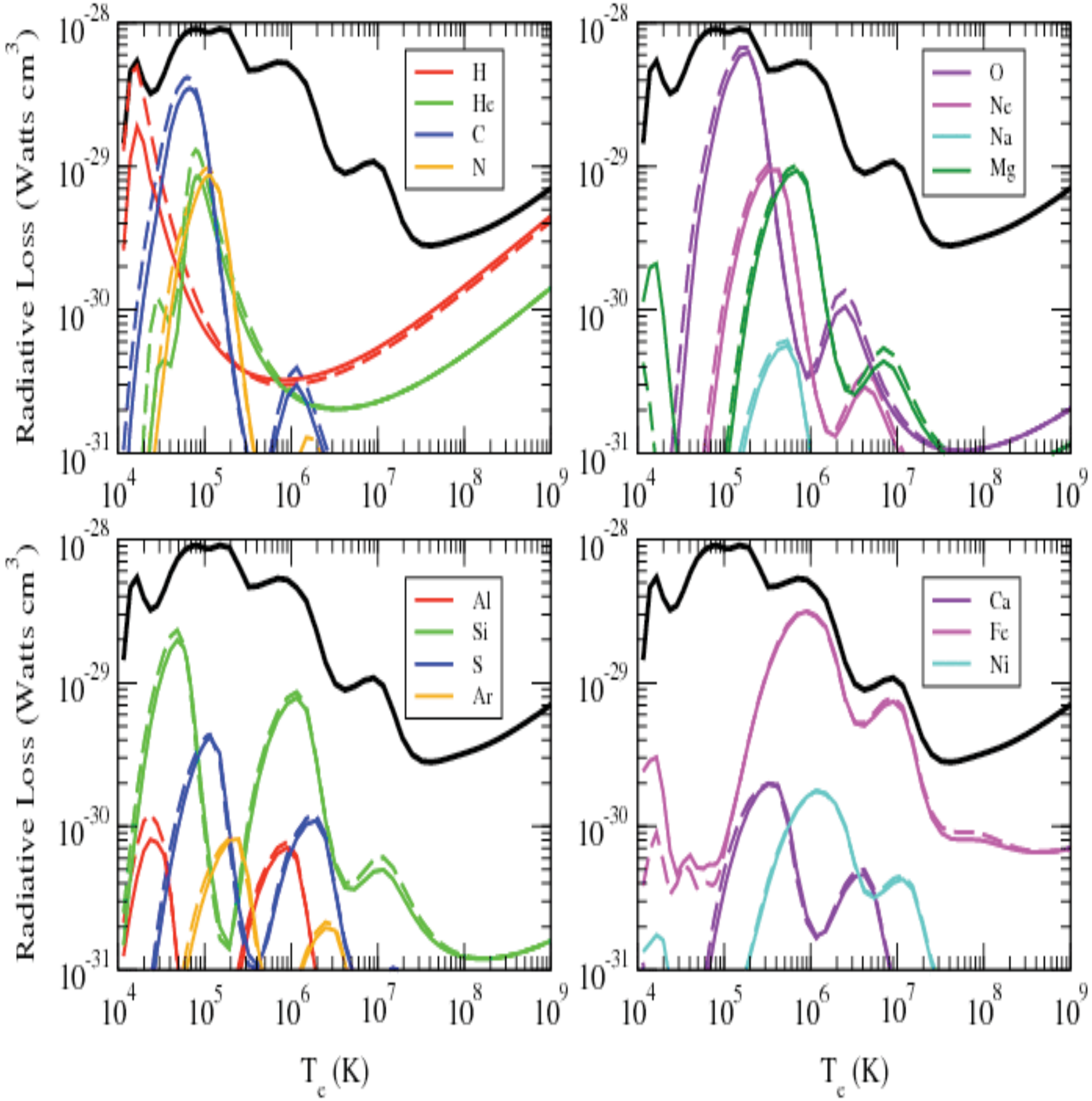

Colgan et al, Astrophysical Journal, 689 585-591 (2008).

Sensitivity to elemental abundances

The previous radiative losses were computed using "quiet region" elemental abundances

Some regions of the corona have different abundances of elements with low (< 10 eV) first-ionization-potentials (FIPs)

These include the elements Na, Mg, Al. Si, Ca, Fe, and Ni

Thus we present the radiative losses for a variety of FIP bias values (relative to the photospheric abundances)

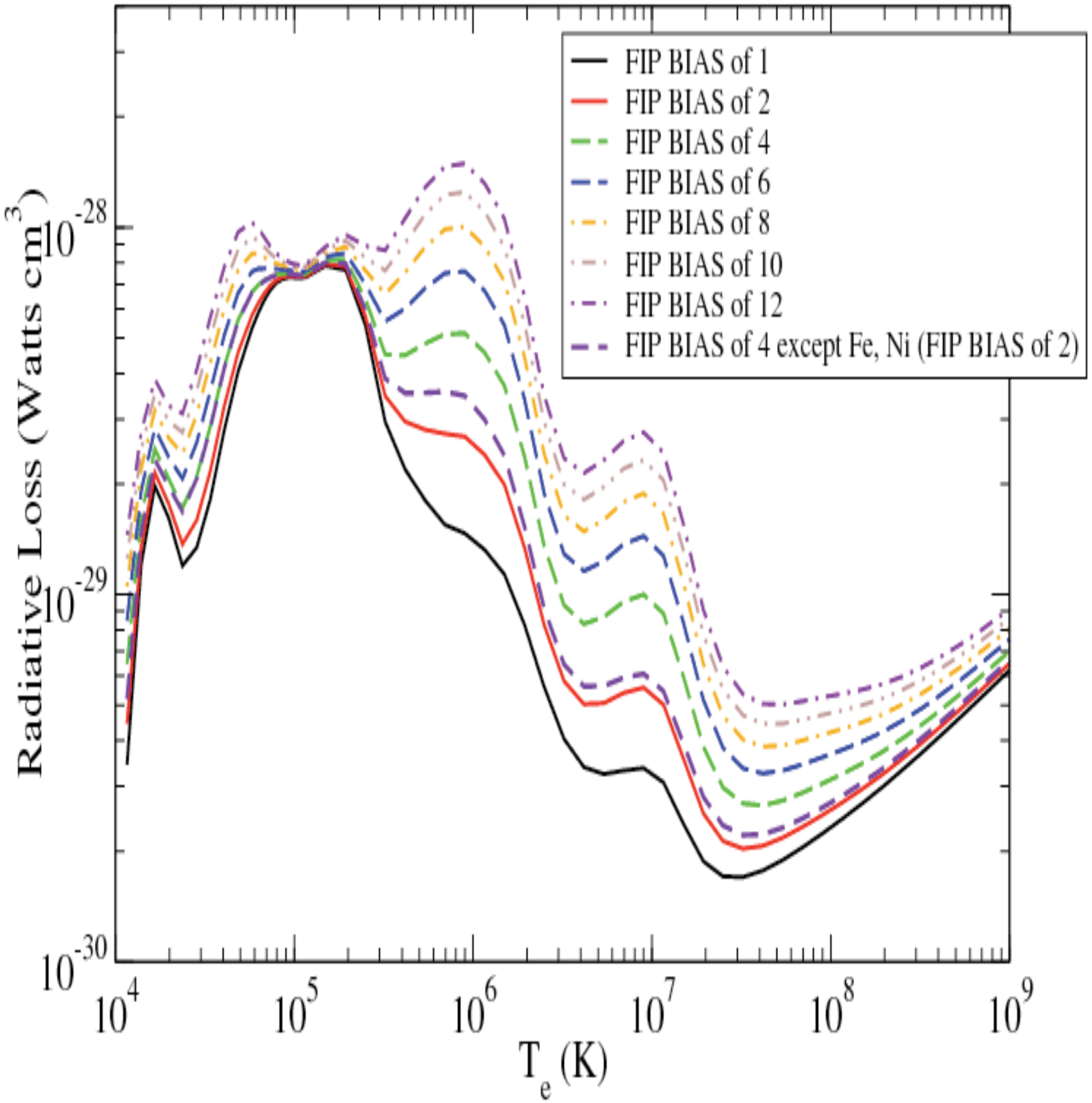

Let’s model L-shell Ge spectra

- Choose configurations
- Run CATS, ACE, and Gipper for energy levels and cross sections
- Guess likely plasma conditions, density and temperature
- Run ATOMIC code
- Iterate

Choosing configurations

- Looking at spectra for excitations from the L shell (n =2).
- For neon-like choose: $2p^6$, $2p^5nl$, $2p^4 3lnl$, $2s^1 2p^6 3l$, $2s^1 2p^5 3lnl$, $2s^0 2p^6 3lnl$, $n \leq 7$, about 200 configurations.
- Choose similar configurations for Mg-like, Na-like, F-like, and O-like.

CR modeling can be used to diagnose plasma conditions. Ge laser produced plasma, Milan, <z> ~ 22, Ne-like. KT =560eV, Ne =10^21. ABDALLAH et. al., Laser and Particle Beams (2007), 25, 245–252, blue calculation, red experiment.

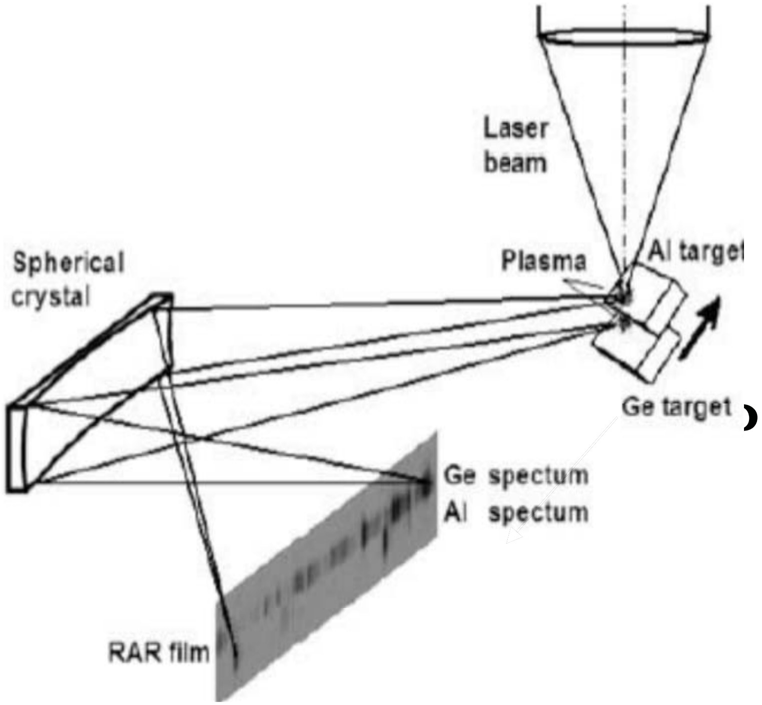

’T

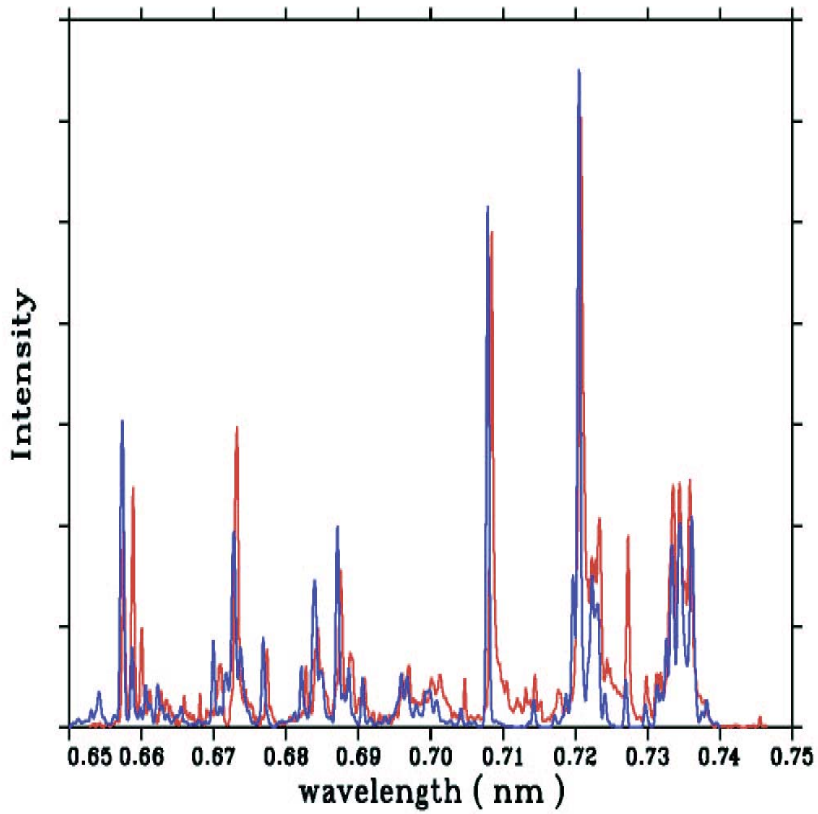

Individual spectral lines can be identified

Table 1. *Transition lines (angstroms)*

	Theory	Experiment
1s) 1s 0.0 2s2 2p6 – 2p) 1p 1.0 2s2 2p5 5d1	6.5717	6.5754
1s) 1s 0.0 2s2 2p6 – 2s) 1p 1.0 2s1 2p6 4p1	6.5744	6.5883
2p) 2p 1.5 2s2 2p6 3p1 – 3p) 2d 2.5 2s2 2p5 3p1 5d1	6.6060	6.6008
2p) 2p 0.5 2s2 2p6 3p1 – 3d) 4f 1.5 2s2 2p5 3p1 5d1	6.6126	6.6120
2d) 2d 2.5 2s2 2p6 3d1 – 3p) 2f 3.5 2s2 2p5 3d1 5d1	6.6223	6.6268
1s) 1s 0.0 2s2 2p6 – 2p) 1p 1.0 2s2 2p5 5s1	6.6548	6.6597
2p) 2p 0.5 2s2 2p5 – 1s) 2d 1.5 2s2 2p4 4d1	6.6993	6.7031
2s) 2s 0.5 2s2 2p6 3s1 – 1p) 2p 1.5 2s2 2p5 3s1 5d1	6.7087	6.7077
2p) 2p 1.5 2s2 2p5 – 1d) 2s 0.5 2s2 2p4 4d1	6.7294	6.7324
2p) 2p 1.5 2s2 2p5 – 1d) 2p 1.5 2s2 2p4 4d1	6.7282	
2p) 2p 1.5 2s2 2p5 – 1d) 2f 2.5 2s2 2p4 4d1	6.7261	
2s) 2s 0.5 2s1 2p6 – 1p) 2p 0.5 2s1 2p5 4d1	6.7367	6.7444
2s) 2s 0.5 2s1 2p6 – 1p) 2p 1.5 2s1 2p5 4d1	6.7391	
2p) 2p 1.5 2s2 2p5 – 3p) 2f 2.5 2s2 2p4 4d1	6.7679	6.7739
2p) 2p 1.5 2s2 2p5 – 3p) 4p 2.5 2s2 2p4 4d1	6.7694	6.7791
2p) 3d 2.0 2s2 2p5 3p1 – 1s) 1f 3.0 2s2 2p4 3p1 4d1	6.8124	6.8048
2p) 2p 1.5 2s2 2p5 – 1s) 2d 2.5 2s2 2p4 4d1	6.8212	6.8227
2p) 2p 0.5 2s2 2p5 – 1d) 2d 1.5 2s2 2p4 4d1	6.8405	6.8408

Carbon mean ion charge: $N_e=10^{17}cm^{-3}$

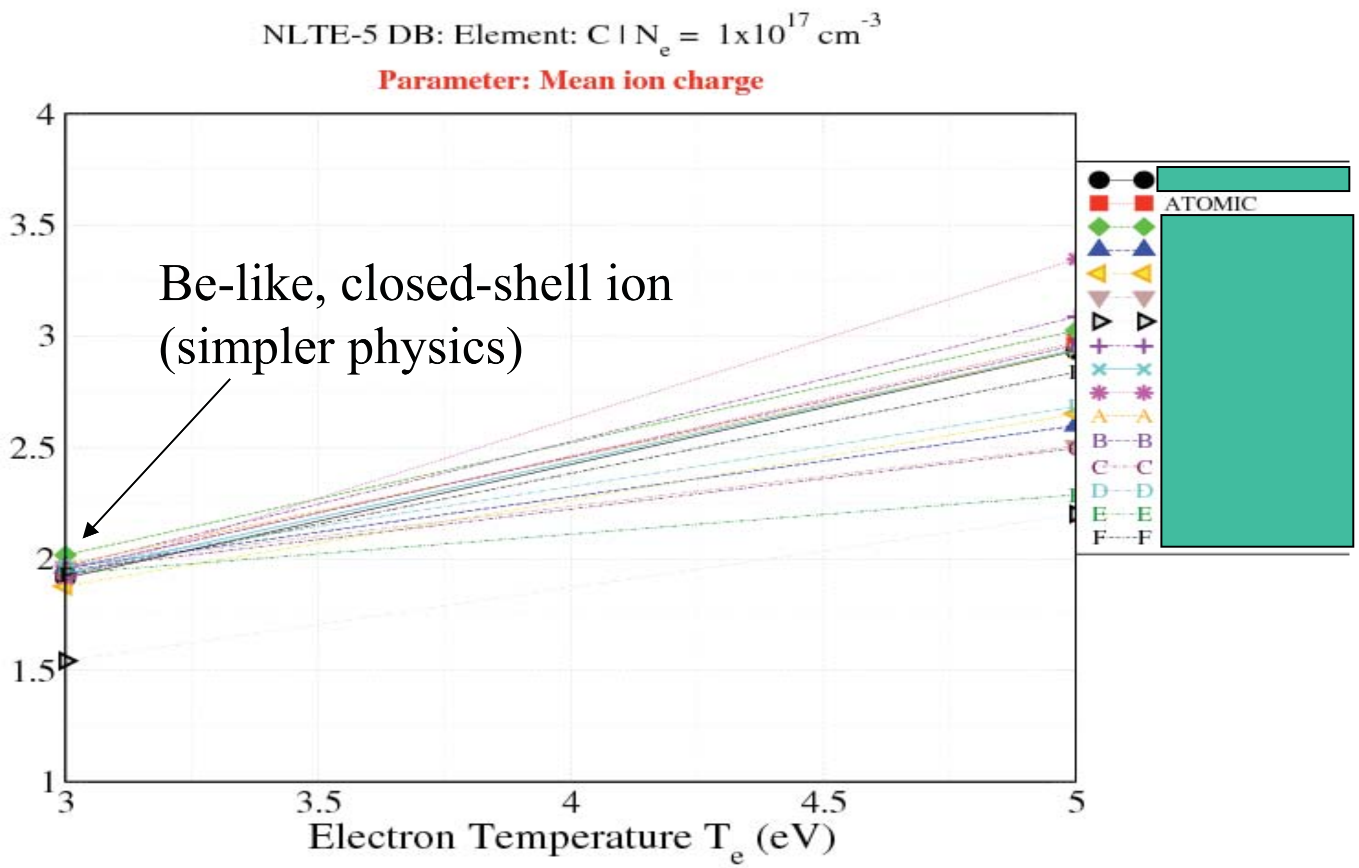

Carbon power loss: $N_e = 10^{17} cm^{-3}$

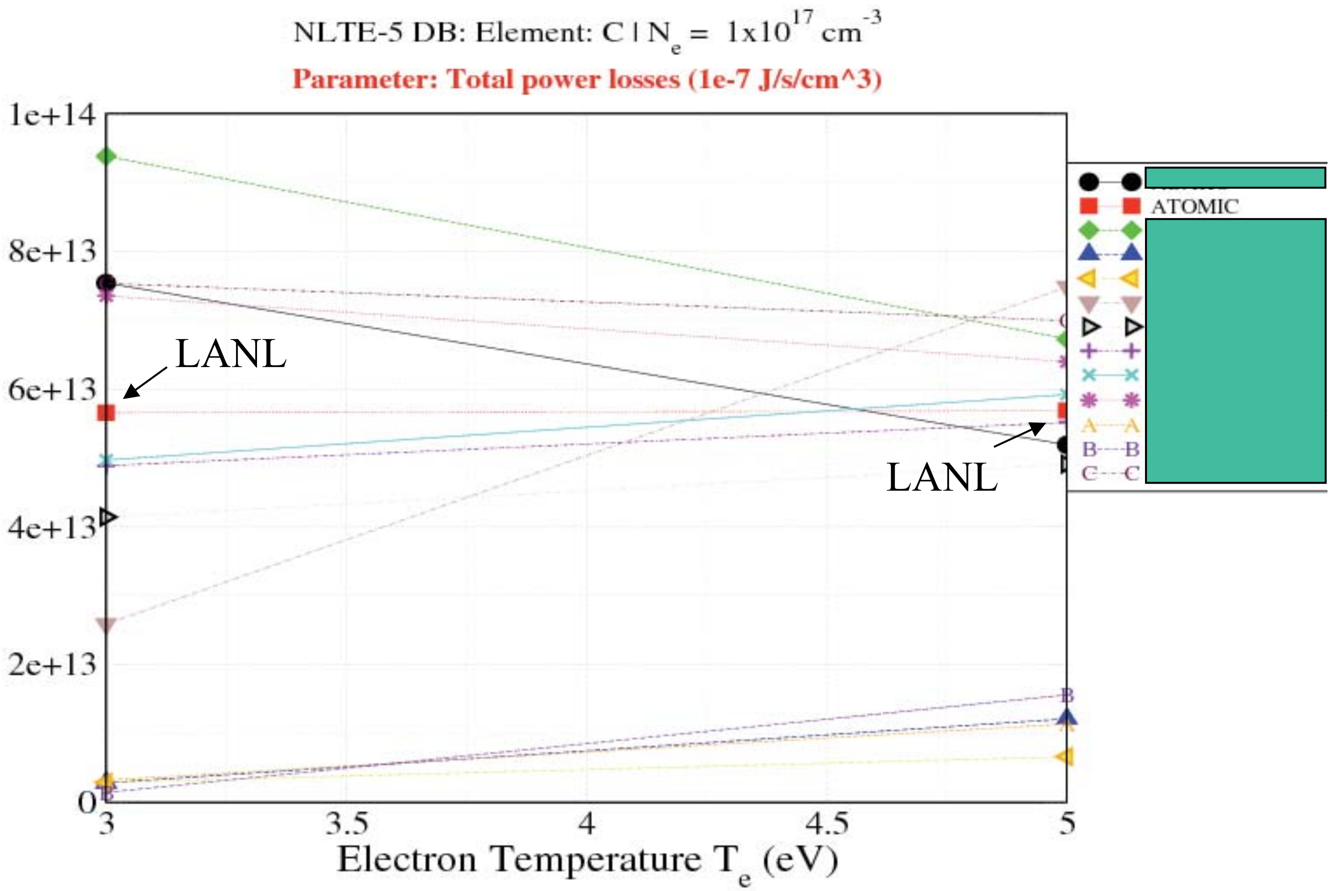

Carbon emissivity: $N_e=10^{17}$ cm^{-3},

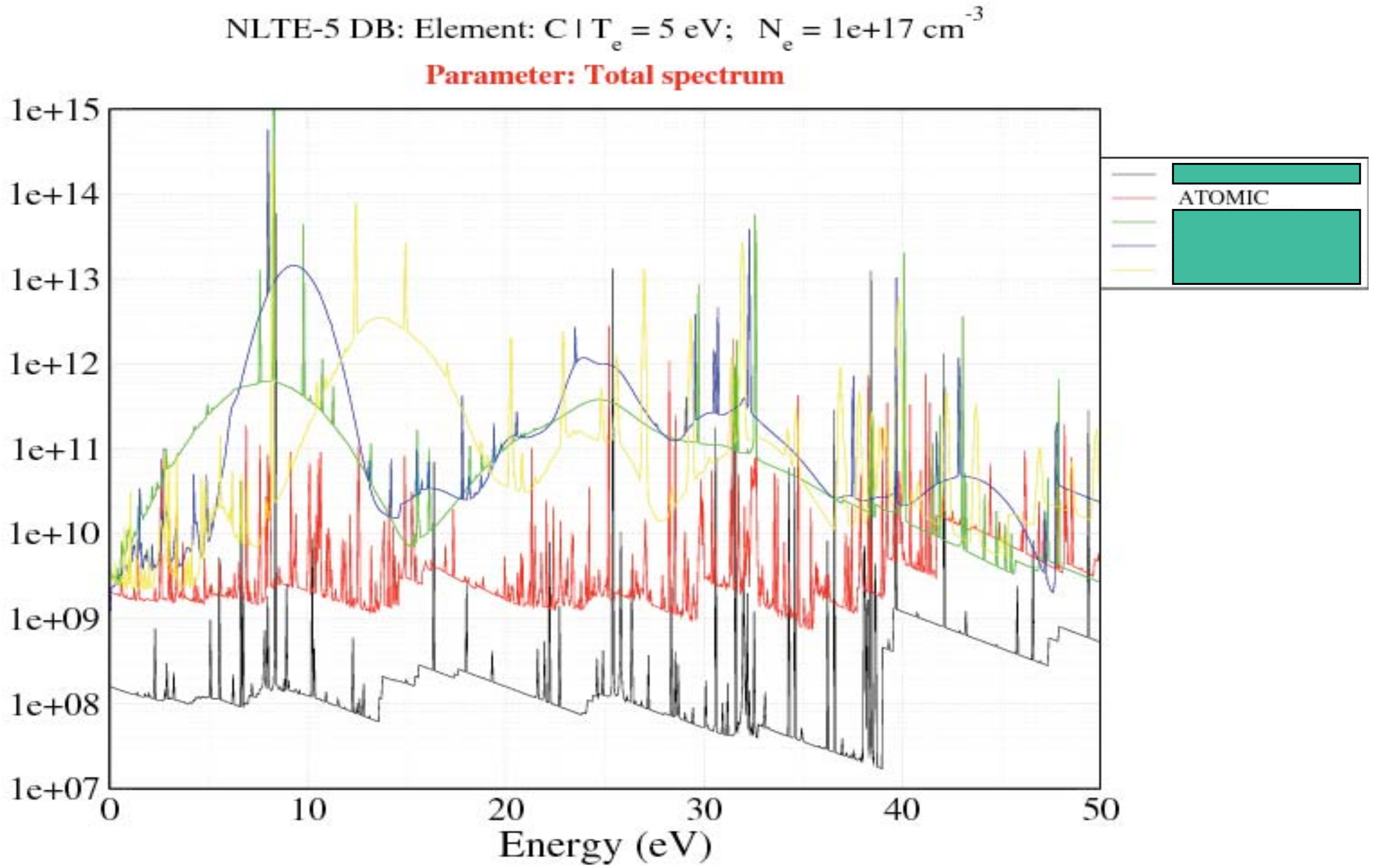

Krypton: radiative loss rates at $N_e=10^{14}$ cm^{-3}

LANL provides only results within error bars

Experimental tokamak data from Fournier et al. Nucl. Fusion 40, 847 (1999)

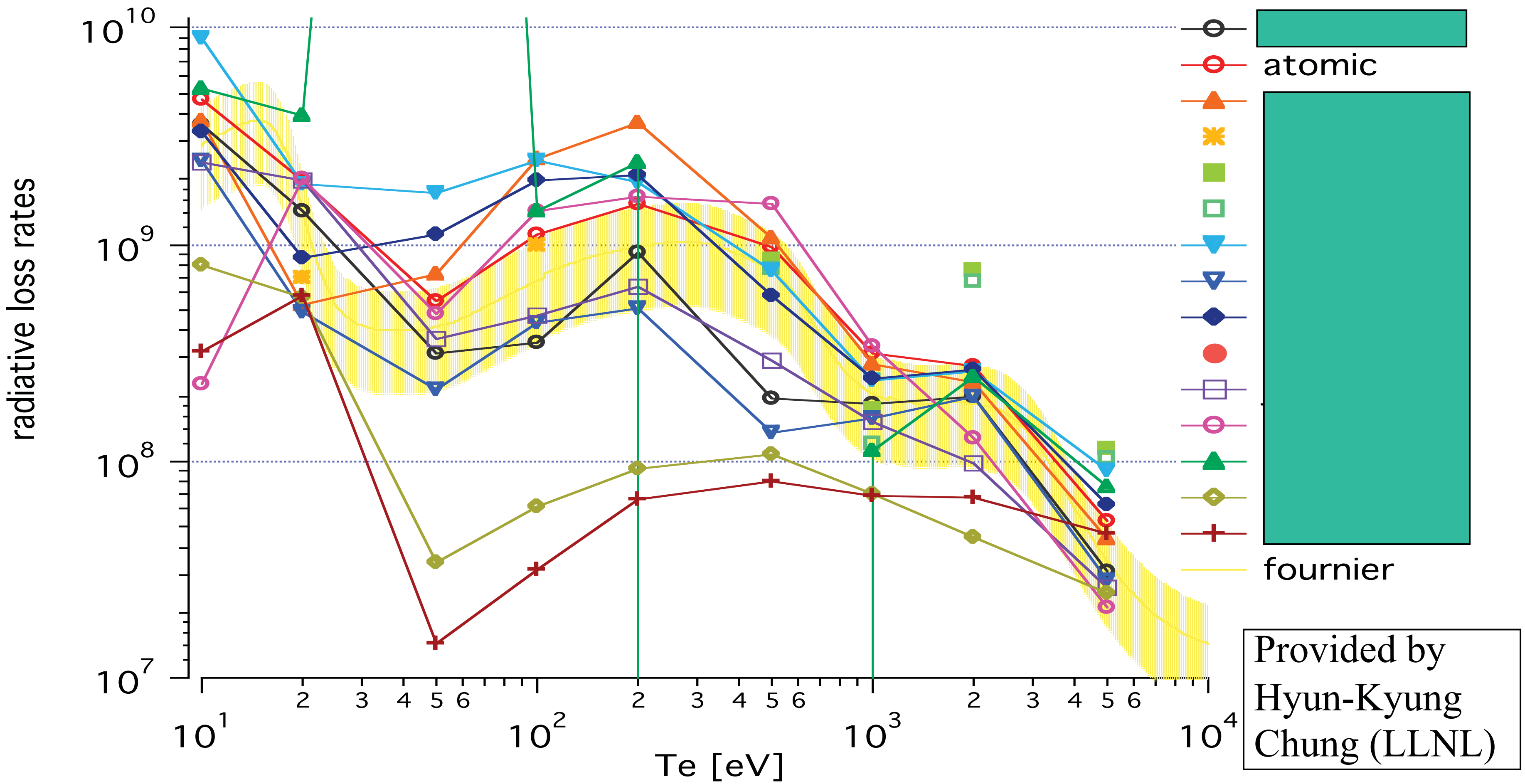

Tungsten: possible ITER wall material

Nuclear Fusion, June 2007: Progress in ITER Physics Basis

500 MW of fusion energy for extended periods of time (x10 more than needed to sustain plasma)
Duration: > 400 s

Currently: **JET 16 MW**

Cost: **5 G€** construction +
5 G€ for 20-year operation

Radius: **6.2 m**
Volume: **830 m^3**
Current: **15 MA**
Density: **10^{14} cm^{-3}**
Temperature: **20 keV**

First plasma: 2016

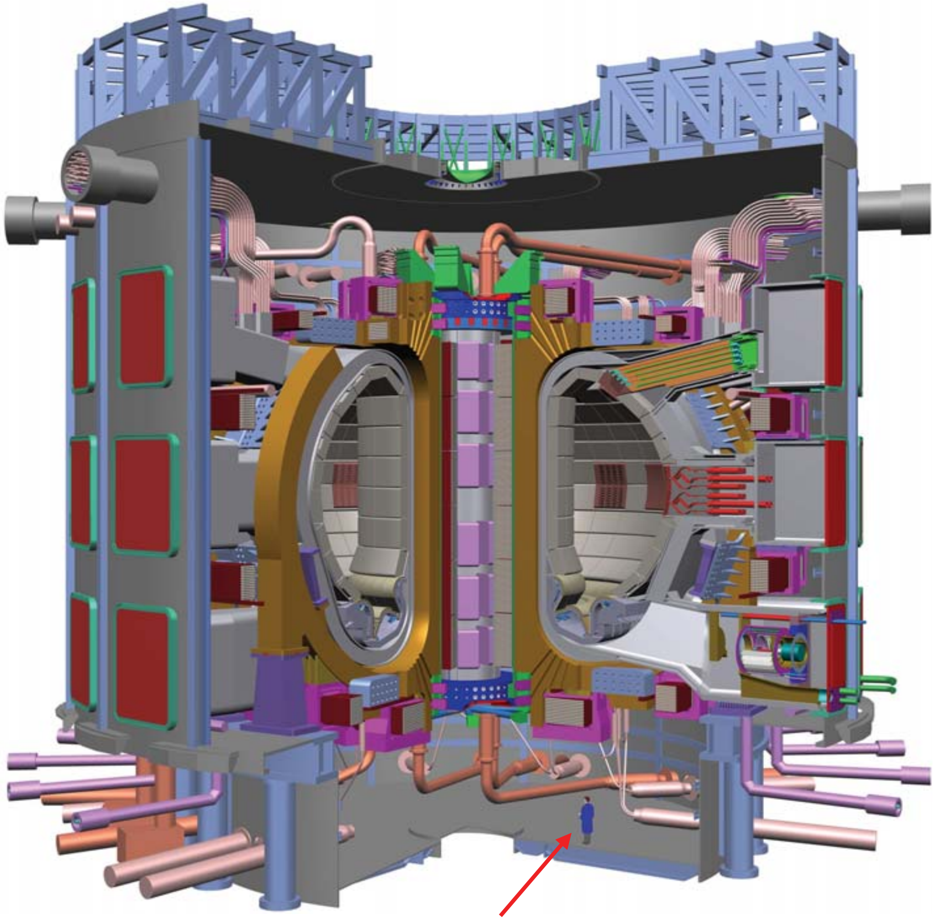

Provided by
Yuri Ralchenko (NIST)

Cross-section of the vessel

- Be
  - Low radiative losses
  - Low plasma contamination
  - Low bulk tritium inventory
  - BAD: low melt temperature
- W
  - Low erosion rate (high sputtering threshold)
  - Low tritium retention
  - BAD: high radiative losses
- CFC
  - High melting temperature
  - High thermal shock and thermal fatigue resistance
  - BAD: high tritium retention

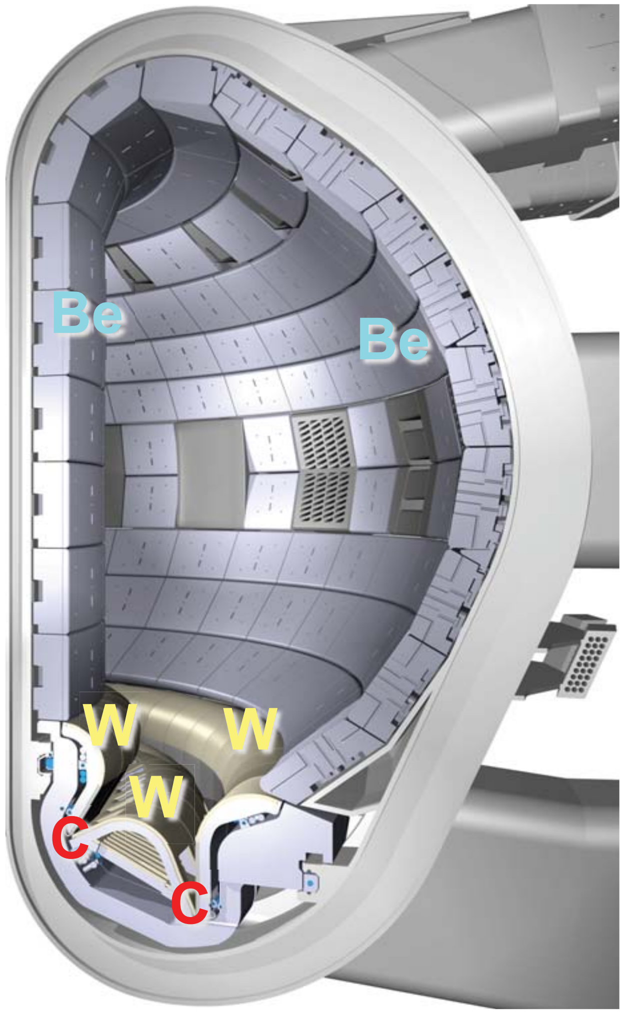

Tungsten mean ion charge for ITER conditions

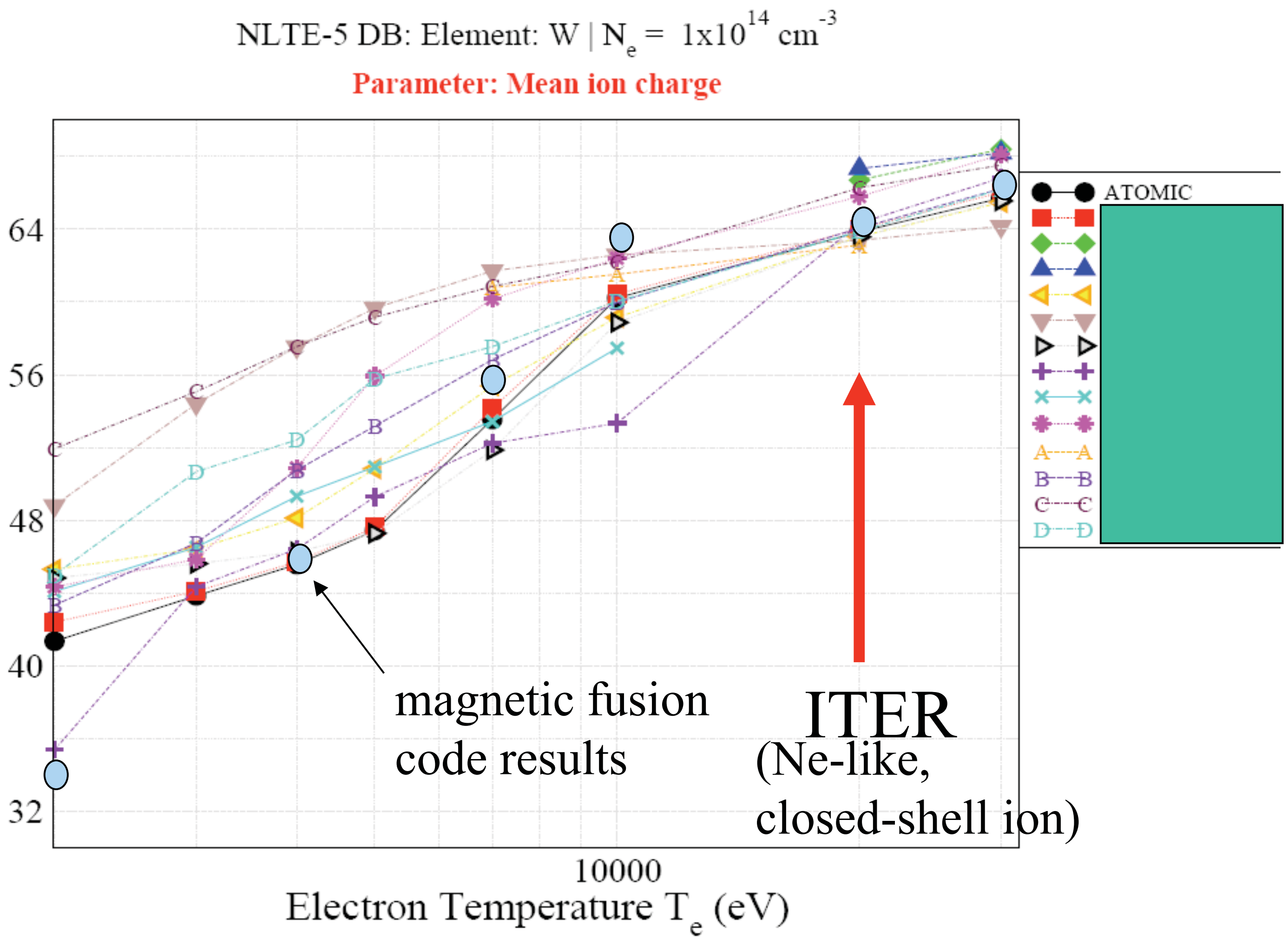

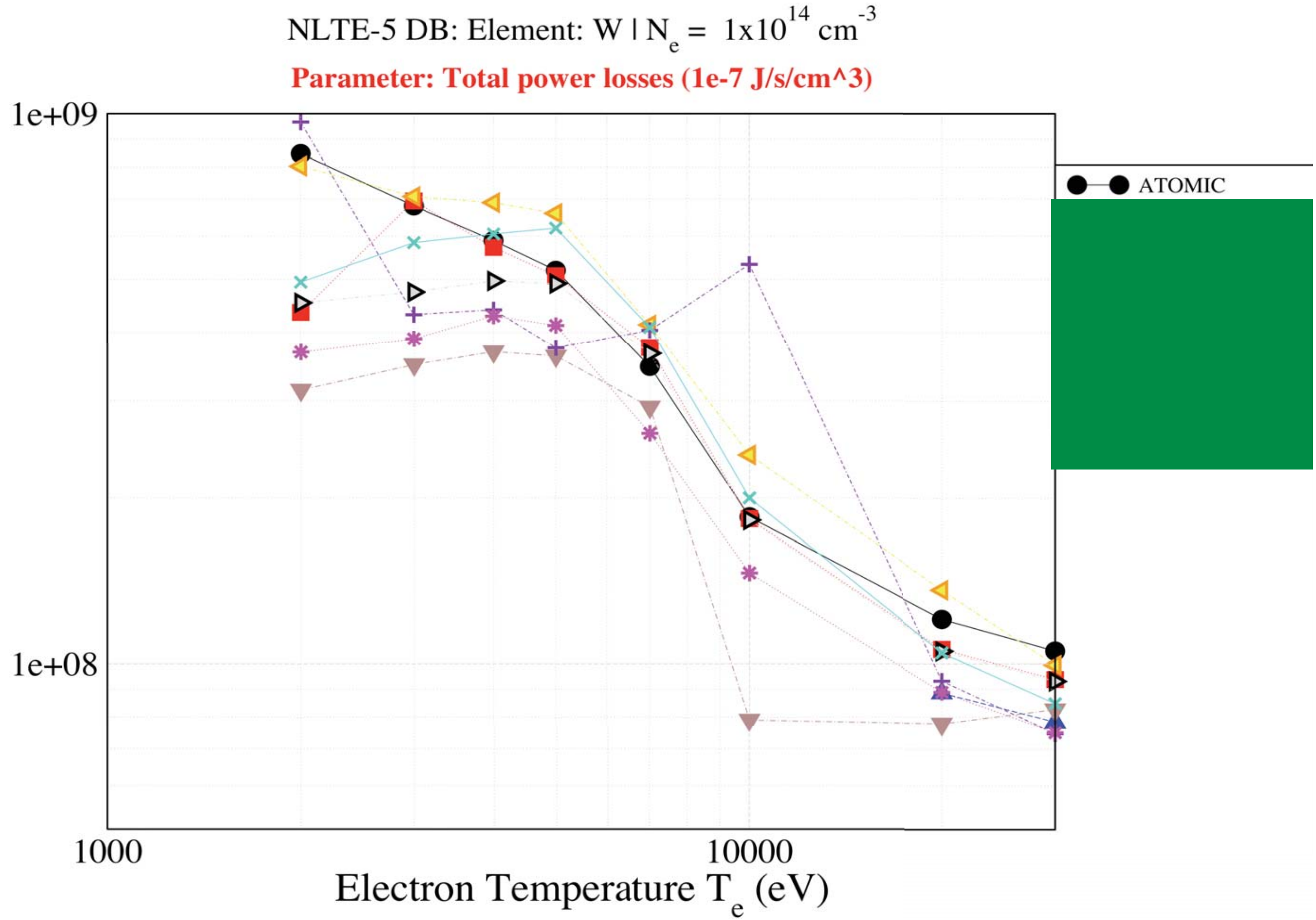

NLTE-5 DB: Element: W | N_e = $1x10^{14}$ cm^{-3}
Parameter: Total power losses (1e-7 J/s/cm^3)
1e+09
1e+08
1000
10000
Electron Temperature T_e (eV)
ATOMIC

What is opacity?

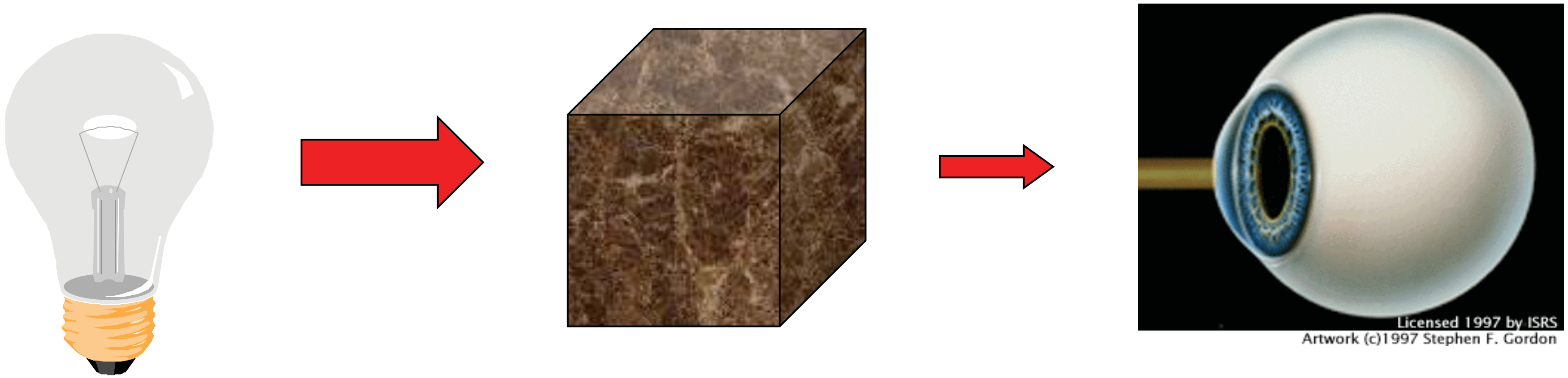

$$\boxed{\frac{\partial I_\omega(x)}{\partial x} = -\kappa_\omega \rho I_\omega(x)}$$

$$\boxed{I_\omega(x) = I_0 \exp\left(-\kappa_\omega \rho x\right)}$$

Applications of Opacities

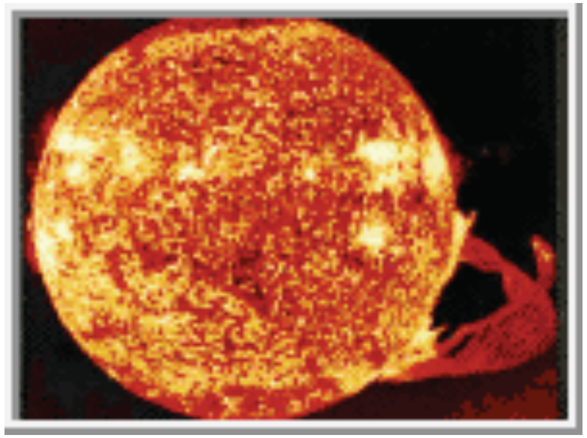

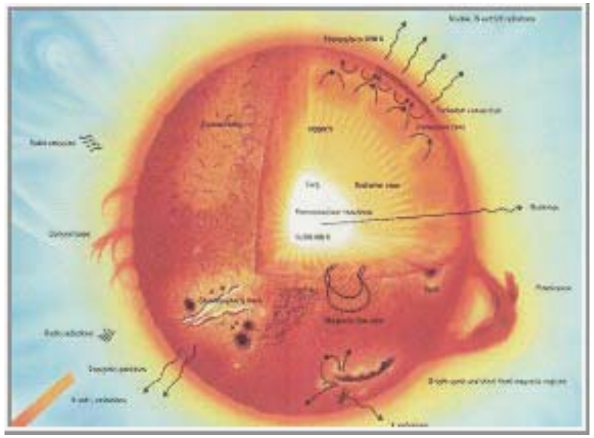

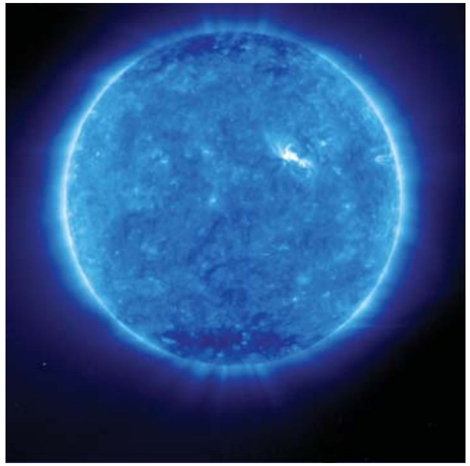

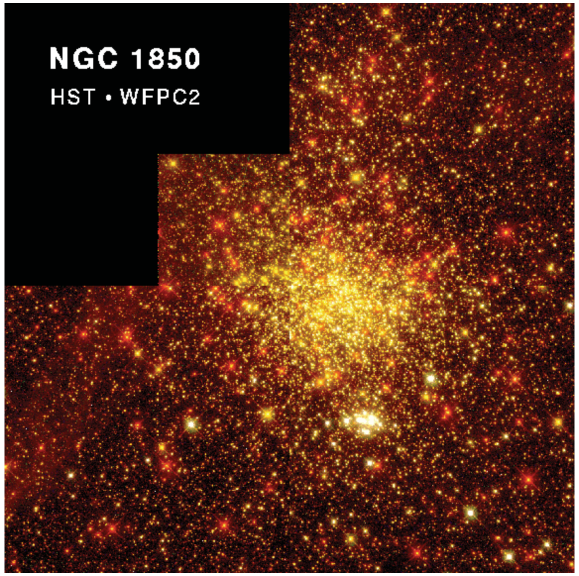

Physical processes contributing to the opacity:

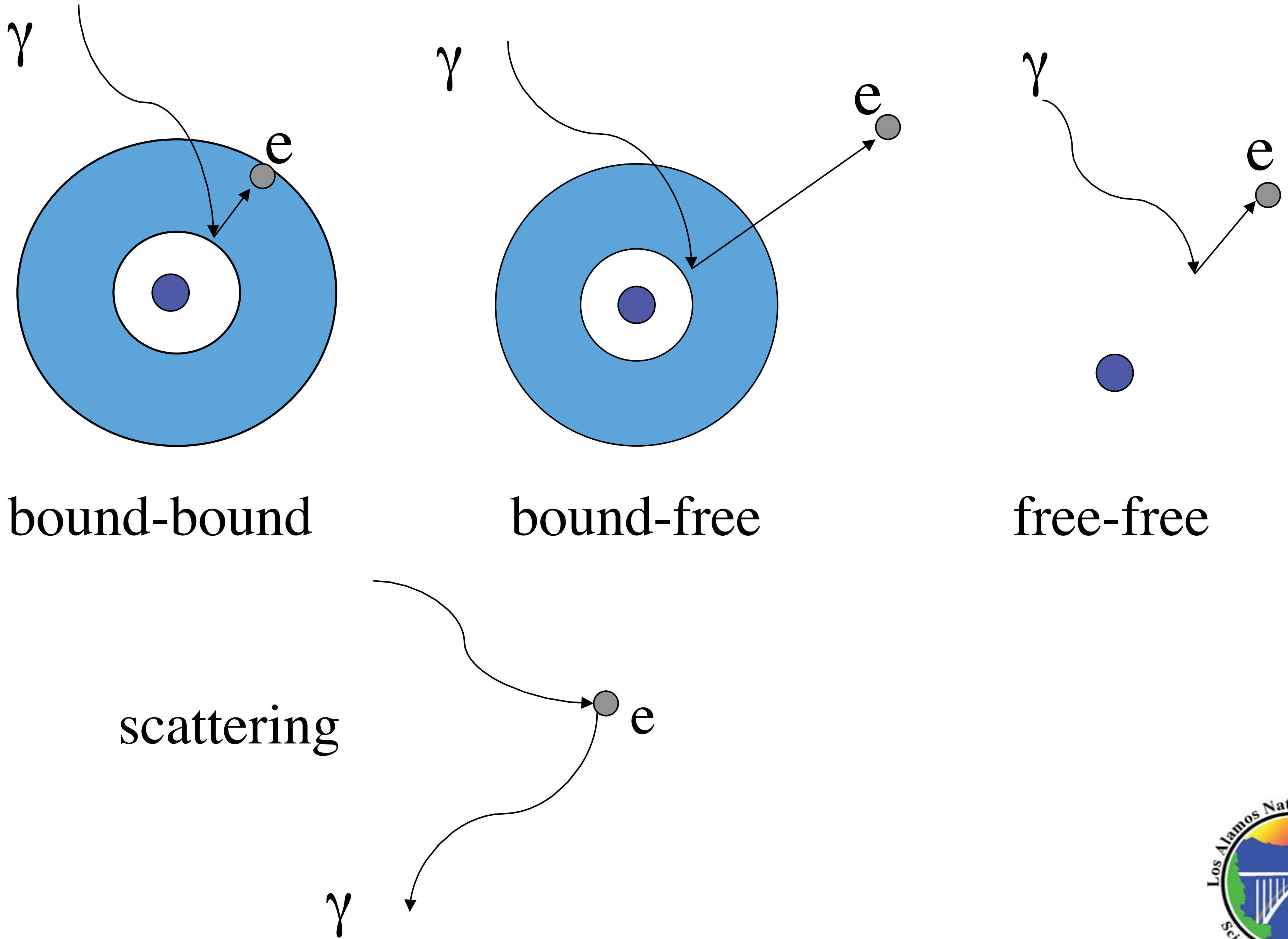

These photon absorption and scattering processes
Combine to give the frequency dependent opacity:

$$\boxed{\kappa_\omega = \left(\kappa_{bb} + \kappa_{bf} + \kappa_{ff}\right)\left(1 - \exp\left(-\hbar\omega / kT\right)\right) + \kappa_s}$$

$$\kappa_{bb} = \frac{1}{\rho} \sum_{il} N_{il} \frac{he^2\pi}{m_e c} \frac{(gf)_{ilm}}{g_{il}} \Phi_{ilm}(h\nu)$$

$$\kappa_{bf} = \frac{1}{\rho} \sum_{il} N_{il} \sigma_{iljm}(h\nu)$$

$$\kappa_{ff} = 4.1 \times 10^{-23} \frac{1}{\rho} \frac{N_e}{T_0^{7/2} (h\nu / kT_e)^3} \sum_i q_i^2 N_i$$

$$\rho = \text{mass density } g(cm)^{-3}$$

$$T_0 = \text{temperature}(^\circ Kelvin)$$

Components of the frequency dependent opacity (bound-bound, bound-free, free-free and scattering)

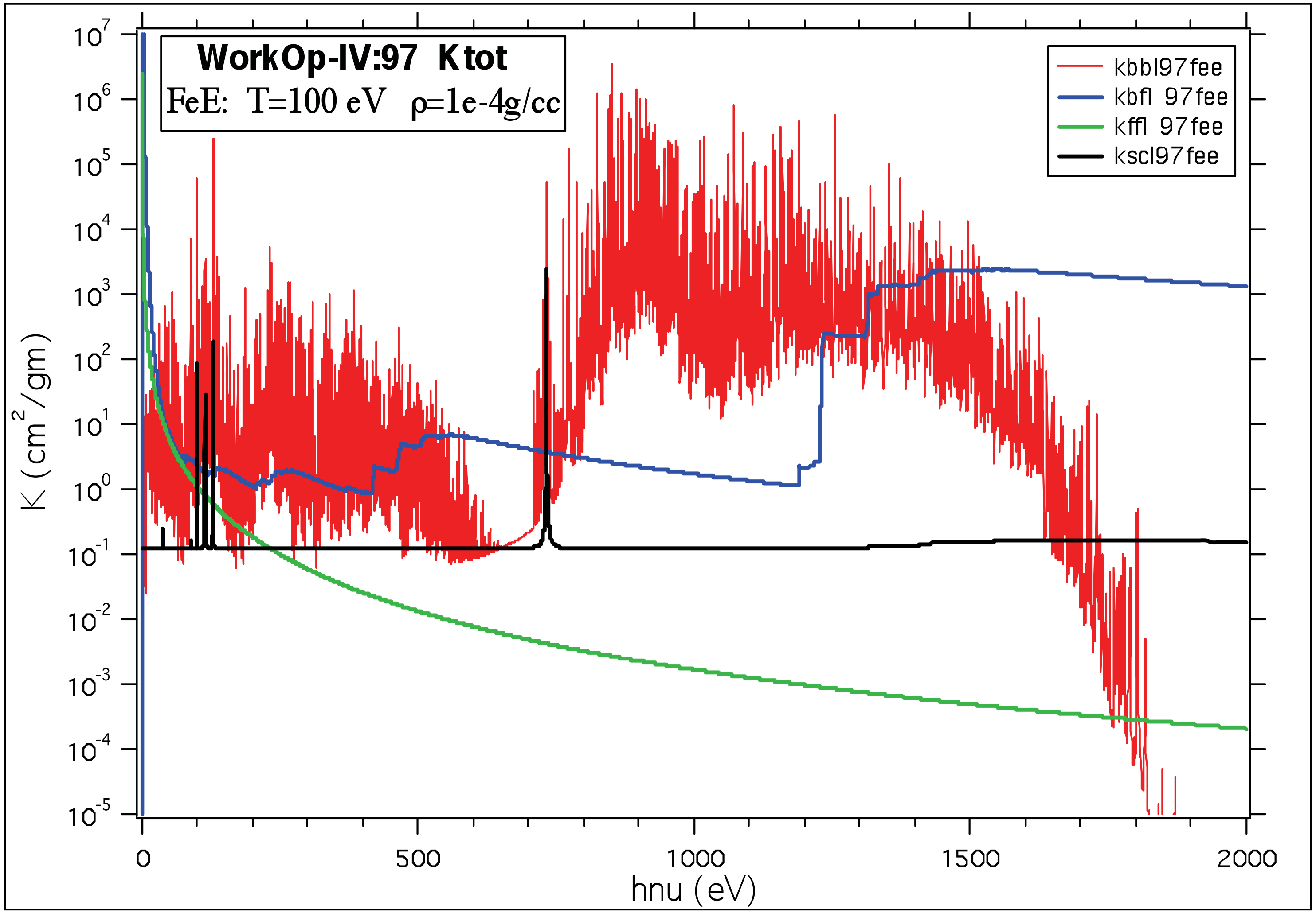

The resultant total frequency dependent opacity

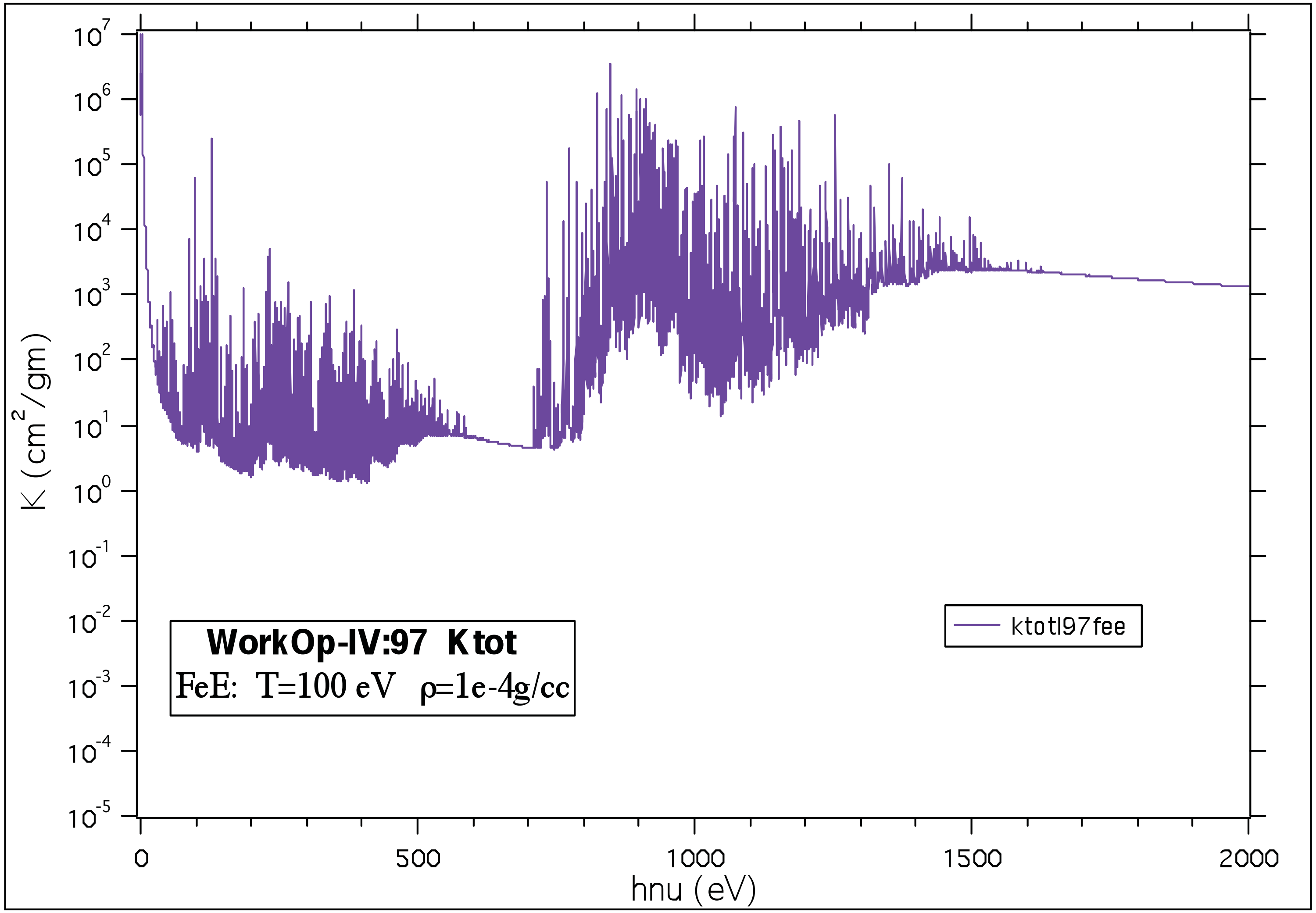

The 20million Amp current provided by the Z accelerator enables this research

Magnetically-driven z-pinch implosions efficiently convert electrical energy into radiation

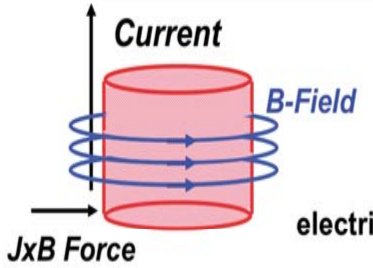

electrical energy
↓
kinetic energy

kinetic and electrical energy
↓
internal (shock heating)
↓
x rays

Initiation

Implosion

Stagnation

- Energy: 1.5 MJ x-ray ≈ 15% of stored electrical
- Power: 200 TW x-ray

Sandia National Laboratories

Laboratory experiments test opacity models that are crucial for stellar interior physics

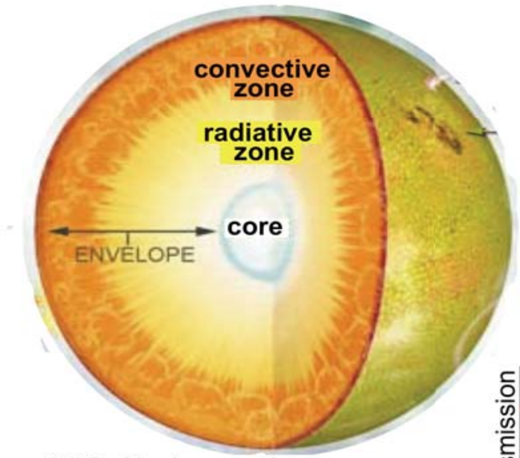

2007 Don Dixon / cosmographica.com

Predictions of solar structure do not agree with observations

Solar structure depends on opacities that have never been measured

<u>Challenge: create and diagnose stellar interior conditions on earth</u>

Z opacity experiments reach T ~ 156 eV

High T enables first studies of transitions important in stellar interiors

Fe / Mg transmission at T ~ 156 eV

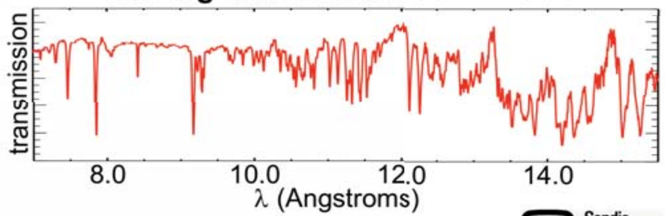

Sandia National Laboratories

Modern solar models disagree with observations. Why?

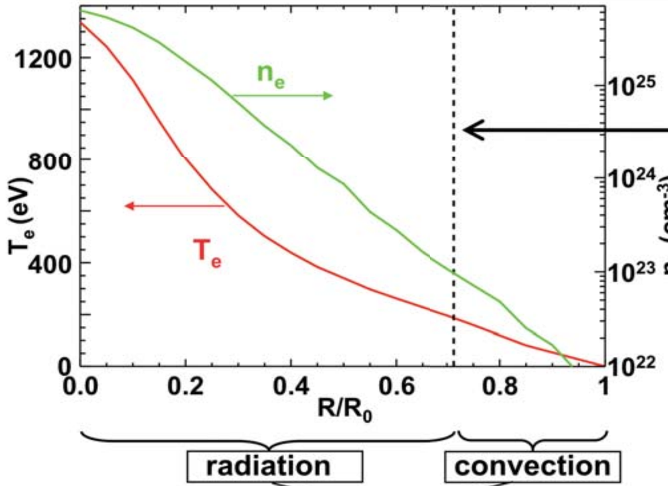

- measured boundary $R_{CZ} = 0.713 \pm 0.001$
- Predicted $R_{CZ} = 0.726$
- Thirteen σ difference

"The CZ problem"

Bahcall et al, ApJ 614, 464 (2004).
Basu & Antia
Physics Reports 457, 217 (2008).

- Boundary location depends on radiation transport
- A 10-20% opacity change solves the CZ problem.
- This accuracy is a challenge – experiments are needed to know if the solar problem arises in the opacities or elsewhere.

Sandia National Laboratories

J.E. Bailey et. Al. Iron opacity measurements at temperatures above 150 eV, Physical Review Letters 99, 265002(2007).

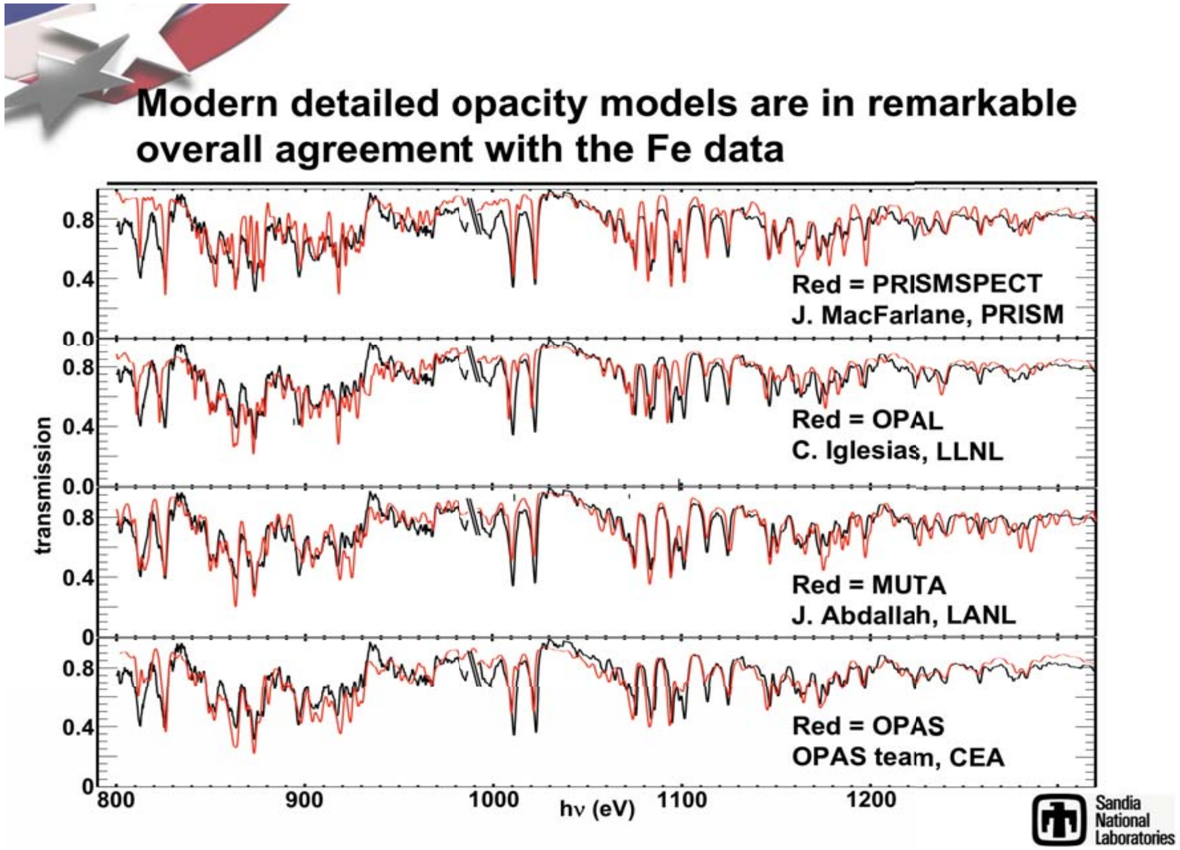

Exercises

(I) Consider the 2 state system. Let $N_1$and N_2 be the population density of the 2 states respectively. Let N = the constant total number density. Let c be the rate coefficient for excitation from state 1 to state 2, d be the de-excitation rate coefficient from state 2 to state 1, and r be the spontaneous decay rate from state 2 to state 1. Let N_e denote a given electron density.

(1)Write down the rate equations for N_1 and N_2 and derive an expression for the steady-populations of both in terms of N.

(2) Derive a formula for N_1 and N_2 as a function of time(t) by directly solving the differential rate equations.

(3) Check the formula to if the steady-result is obtained as t gets large, also check the formula for N_e small (coronal limit), and for large N_e (LTE).

(4) Derive an expression to first order for the relaxation time, the time it takes for N_1 to reach its steady-state value.

Exercises

(II) Assume the 2-level system of the previous example to be the 1s and 2p configurations of H-like Lithium. This example is actually of interest in Lithography because of its wavelength. Calculate the power (Watts/cm^3) emitted by the 2p-1s emission line at N=?, N_e=? and kT_e=?. Use the LANL atomic physics website to evaluate the required atomic data.

(III) Use the LANL atomic physics website to identify the major lines observed in the following O spectra shown . Match the observed line position with calculated values. Use the assumption of LTE to estimate the temperature from selected line ratios.

Exercise III